BACTERIOPHAGE-BASED BIOCONTROL OF THE BIOFILM FORMED BY ANTIBIOTIC-RESISTANT BACTERIUM

by

Ran Jing

A thesis submitted to the faculty of
The University of Utah
in partial fulfillment of the requirements for the degree of

Master of Science

Department of Civil and Environmental Engineering

The University of Utah

August 2012

Copyright © Ran Jing 2012

All Rights Reserved

The University of Utah Graduate School

STATEMENT OF THESIS APPROVAL

The thesis of **Ran Jing**

has been approved by the following supervisory committee members:

Ramesh Goel	, Chair	**4/24/2012** Date Approved
Andy Hong	, Member	**4/24/2012** Date Approved
Otakuye Conroy-Ben	, Member	**4/24/2012** Date Approved

and by **Paul Tikalsky**, Chair of the Department of **Civil and Environmental Engineering**

and by Charles A. Wight, Dean of The Graduate School.

ABSTRACT

Antibiotics are not only essential for human health but also for the well-being of plants and animals. However, the use of antibiotics has led to the evolution of antibiotic-resistant bacteria (ARB) in the environment. Antibiotic resistance in bacteria is a serious public health concern. ARBs are not only a predicament in clinical scenarios and daily life but also existing in many other environments. Wastewater treatment plants have been acknowledged as breeding grounds for such bacteria. As part of this research, a kanamycin-resistant bacterium, *Chryseobacterium taeanense strain K-2,* was isolated from the Central Valley Water Reclamation Facility and chosen as a model organism for the study. The bacterium was Gram negative, 0.5 μm long with coccoid morphology, and belonged to the *Flavobacteriaceae* family. The doubling time was observed to be ~2 h. Some species of bacteria under this genus have been associated with pathogenicity in human. This is, however, the first report on an antibiotic-resistant strain of *Chryseobacterium taeanense* and its presence in wastewater can be a serious concern.

A lytic bacteriophage infecting *Chryseobacterium taeanense strain K-2* was isolated from Central Valley Water Reclamation Facility. The lytic infection was evident from distinct clear plaques of 1-2 mm diameter obtained on top agar plates. According to the TEM analysis, the phage belongs to the *Podoviridae* family with a short tail,

hexagonal head, and a total length of 90-100 nm. The latent and eclipse period of lytic infection were found to be the same (10 min). The burst size was around 18 ± 2 PFUs/infected cell.

Significantly short latent period and relatively high burst size indicate the exceptional potential of the lytic phage to regulate even very high populations of the host. The optimal phage-to-host ratio for infection was found to be 100:1, causing 98.7% of host death after 9 h.

The lytic phage was also found to infect the host cells within the biofilm. The biofilm disintegration and degradation of the extra-polymeric substance within the matrix of the biofilm was evident after overnight infection with the phage. In conclusion, the lytic phage isolated in the present study can be attributed with significant potential for biocontrol of both biofilm-forming and planktonic forms of antibiotic-resistant bacterium, *Chryseobacterium taeanense strain K-2*.

TABLE OF CONTENTS

LIST OF FIGURES

page

LIST OF TABLES

Table Page

ACKNOWLEDGMENTS

Thank you, in particular, to the chair of my committee, Dr. Ramesh Goel. He always encouraged me and gave a constructive criticism, and spent time to answer my questions with great patience. His advice and guidance were completely invaluable. Also, I want to thank Dr. Shireen Meher Kotay. He has given significant insight and future vision to my project.

I would like to thank Choi Jeongdong, Amir M. Motlagh and Ananda Shankar Bhattacharjee for providing advice for the project. Moreover, I am grateful for Dr. Sherwood Casjens's research group for allowing and helping me to do the bacteriophage CsCl purification.

CHAPTER 1

INTRODUCTION

1.1 Antibiotic-resistant bacteria (ARB) in the environment

Antibiotics are drugs which can be used to treat or prevent disease and infections caused by bacteria and other organisms. During the past 60 years, antibiotics played a significant role in fighting against infections caused by bacteria and other microbes. Also, antimicrobial therapy is the most possible explanation of the increase in the average life expectancy. Due to the invention of antibiotics, some diseases and infections can now be easily cured within a few days. However, recently, the unrestrained usage of antibiotics has become a public health problem. Due to excessive use, large amounts of antibiotics are discarded and added to human medicine, agriculture, aquatic and several other natural environments (Huang et al. 2001). Some bacteria present in these environments resist antibiotics by modifying their genetic makeup, a process termed as mutation. These mutations are carried across generations and eventually develop into potent (sometimes multi-) antibiotic-resistant populations. In 1998，in the United States, 12,500 tons of antibiotic prescriptions were used for human beings (Kutateladze et al. 2010). Also, over 60% of antibiotics usage in the U.S was for agricultural practice, adding an additional 18,000 tons per year to the antibiotic burden in the environment.

It is said that about 70 % of the bacteria that caused infections in hospitals can be resistant to more than one common antibiotic drug used for the treatment. In addition, some bacteria can be resistant to all approved antibiotics and the infection caused by these bacteria can only be treated using potentially toxic drugs. In case of community acquired infections, some bacteria have been reported to have antibiotic resistance, such as the Staphylococci and Pneumococci. One of the recent studies (Bisht et al. 2009) indicated that 25% of bacterial pneumonia cases were resistant to penicillin, and 25% of other cases were reported to be resistant to multiple antibiotics. Antibiotic-resistant bacteria and genes have been detected in wastewaters, and the concentrations are higher than that found in surface waters (Börjesson 2009). Antibiotics and their products can be introduced into wastewater or natural environment by humans or animals (Levy 2002). The antibiotics can become a selective pressure for maintaining resistance among microorganisms. Due to the favorable conditions (high nutrients), wastewater treatment plants can support luxuriant growth of ARBs. Furthermore, the antibiotic resistance can be easy to spread across bacteria due to diverse bacterial communities that harbor the wastewater systems. These ARBs can enter/re-enter the ecosystem through receiving water-bodies (rivers, streams, oceans, lakes etc.). Thus, the wastewater system has a major role to play in the emergence and spread of antibiotic resistance within bacterial populations. It also has a potential for working as a model in the development and biocontrol of the antibiotic-resistant bacteria.

Bacteria can gain resistance through two primary means: mutation, and swapping

DNA by using built-in design features (horizontal gene transfer) to share resistant genes from other microorganisms. Antibiotics can kill bacterial cells by disrupting a critical function. The antibiotics specifically bind to some bacterial cell proteins, which are involved in copying the DNA, making proteins, or making the bacterial cell wall, important for the bacteria to grow and reproduce, causing the failure of the protein's functions. If there are mutations in the bacterial genomic DNA, which code for these proteins, the antibiotic cannot bind to the proteins and the bacteria will survive. Therefore, in the presence of antibiotic, the mutant bacterial cells will predominantly survive. On the other hand, bacteria can get antibiotic resistance by gaining the mutant DNA from other bacteria; this phenomenon is termed horizontal gene transfer (Kay et al. 2002). The horizontal gene transfer often involves plasmids (Naik et al. 1994) where the genes specifically coded for antibiotic resistance in one species of bacteria can be transferred to another species of bacteria. In this case, the process requires an environment with genetic diversity and natural selection as the driving forces guiding bacteria resistance to antibiotics.

1.2 Biofilms and biofilms formed by ARBs

Biofilms are microbial communities in polysaccharide-rich extracellular matrices and living in association with surfaces (Pace 2006). As a normal mechanism for bacteria to survive in the environment, when they are exposed to surfaces with a sufficient amount of nutrients, biofilms are formed. The polysaccharide layer is created to protect from the

harmful environments and provide the optimal growth conditions for the survival of bacterial cells. For example, some external biofilms, namely chronic wounds and dental plaque, can be manually removed. Because of their inaccessibility and heightened resistance to certain antibiotic combinations and dosages, internal biofilms are more difficult to eradicate. Researchers have estimated that 60-80 % of microbial infections in the body are caused by bacteria growing as a biofilm – as opposed to planktonic (free-floating) bacteria. Biofilms spreading along implanted tubes/wires, prosthetic limbs or catheters can lead to pernicious infections in patients. In industrial environments, biofilms can develop on the interiors of pipes and lead to clogs and corrosion. Biofilms on floors and counters can make sanitation difficult in food preparation areas.

The mechanism of biofilm-formation is a complex process; in general, the whole process consists of nine steps, as depicted in Figure 1 (Simoes et al. 2009):

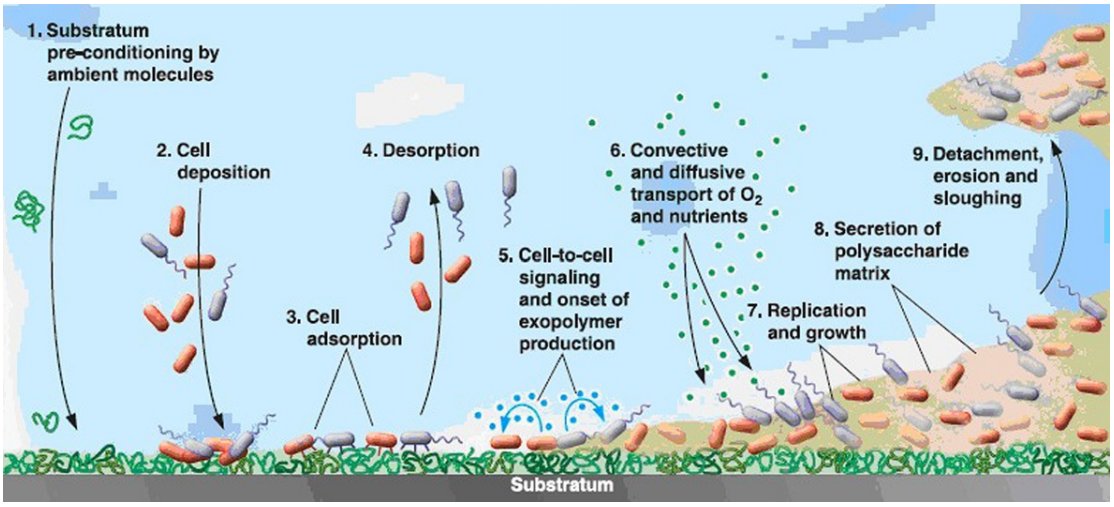

Figure 1: Processes governing biofilm formation (Breyers & Ratner, 2004).

i) Preconditioning of the adhesion surface;

ii) Transport of planktonic cells from the bulk liquid to the surface;

iii) Adsorption of cells at the surface;

iv) Desorption of reversibly adsorbed cells;

v) Irreversible adsorption of bacterial cells at a surface;

vi) Production of cell–cell signaling molecules;

vii) Transport of substrates to and within the biofilm;

viii) Substrate metabolism by the biofilm-bound cells and transport of products out of the biofilm. These processes are accompanied by cell growth, replication, and EPS production;

ix) Biofilm removal by detachment or sloughing.

Initially, free-floating antibiotic resistant bacterial cells attach to a surface through weak van-der-Waals forces and anchor to the surface permanently using cell adhesion molecules. These first colonists as initial adhesion sites will promote more and other bacterial cells to arrive and begin to build the matrix that holds the biofilm together. The matrices can provide a protection and promote communication among the cells through chemical and physical signals. It is known that some biofilms' matrix contain water channels that help distribute nutrients and signaling molecules (Haggag 2010). Some bacterial species can attach to surfaces on their own. Others are able to attach to the matrix or earlier colonists. Once colonization finishes, these bacterial layers will develop into larger cell clusters and create the structures of biofilm by combination of cell

division and recruitment.

It is noticed that bacteria in biofilms have significantly different properties from free-floating bacteria. The cells are dense as a protected environment that allows them to cooperate and interact. The benefit of dense cells is that the outer layer of cells and extracellular matrix protect the interior of the community to increase resistance to antimicrobials and antibiotics. The benefit of dense cells is that the outer layer of cells and extracellular matrix protect the interior of the community to increase resistance to antimicrobials and antibiotics. In other words, it is not all biofilm cells represent highly resistant, biofilms' antibiotic resistance can be determined by the susceptibility of the most resistant cell.

On the other hand, ARBs that grow as adherent biofilms are more difficult to eliminate. ARBs can possibly reside in biofilms and lead to enhanced tolerance to adverse environmental conditions, causing serious infectious diseases (Ngwai et al. 2006). ARBs can resist even high doses of antimicrobial drugs, making traditional therapeutics obsolete. Moreover, the antibiotic-resistant pathogens can exist in the form of biofilms, leading to cross-resistances to other environmental stresses (Gilbert et al. 2002). However, there is a lack of information on the biofilm-associated infections involved in altered virulence properties of antibiotic-resistant bacteria. Relatively few studies have been focused on the biofilm-forming abilities of multiple antibiotic-resistant pathogens. The biofilm formation by multidrug-resistant pathogens may increase the risk of severe infections related to food processing facilities and medical devices.

1.3 Current therapeutics for ARB biofilms

Prevention strategies for antibiotic resistance are essential to control the spread of antibiotic-resistant pathogens. However, the discovery and development of novel antibiotics has lagged behind the emergence of antibiotic-resistant pathogens because of the lengthy and expensive processes, requiring phases of clinical investigation trials to obtain approval, and the lack of information on the antibiotic resistance mechanisms. Drugs like linezolid and daptomycin with novel modes of action were developed and approved (Fischbach and Walsh 2009). However, just a few years after their introduction into the market, clinical strains resistant to those antibiotics were reported. These observations imply that the traditional approach of antibiotic discovery, though highly successful in the introduction of numerous drugs, cannot sustain the high demand for development of novel compounds (Breithaupt 1999). Therefore, a more efficient antibiotic discovery platform is essential for allowing us to compete with the evolution of microbial resistance (Davies 1994). In the post-genomic era, with the availability of various genomics-based platforms including whole-genome sequencing, genotyping, and gene expression profiling, a new horizon opens that could revolutionize our pursuit of novel antimicrobial agents (Amini and Tavazoie 2011).

However，there are still many limitations when these therapeutics are applied to control biofilms formed by antibiotic-resistant bacteria. For example, chemicals can pass over the surface of a biofilm and only affect bacteria at that surface instead of penetrating the biofilm and the EPS matrix. Biofilms can form layers and matrices that can decrease

the activity of chemical treatment to the point where effective concentrations cannot be achieved. Hence, it is required that biocides must be mobile so they can migrate to the film surface and across the bacteria cell membrane to destroy bacteria.

Moreover, the emergence of resistant bacteria to conventional antimicrobials results in a large amount of antibiotics use, demonstrating that novel biofilm control strategies are required. Novel drug delivery technologies have been studied as targets for controlling the process of biofilm formation. To prevent colonization, this technology combines devices of surface modification with biofilm development along with antimicrobials. Electrical approaches are used to release antimicrobials from device surfaces or introduce antimicrobials through the biofilm (Smith 2005). Other therapeutics, such as liposomal systems, have been used to aim antibiotics onto the biofilms' surface, or to target antibiotics towards intracellular bacteria. In addition, new concepts in case of a polymer-based carrier such as biodegradable polymers has been proposed. Phage therapy can help to control biofilm by killing bacteria either before they are able to attach to a surface or before they proliferate. Hence, bacteriophages might provide a possible natural, highly specific, nontoxic way for controlling biofilm formation (Kudva, Jelacic, Tarr, Youderian, and Hovde 1999).

1.4 Bacteriophages

Bacteriophages are viruses which can infect and kill a specific bacterial host. Bacteriophages cannot replicate independently without a living host cell. Therefore,

bacteriophages enter into a suitable living cell and utilize energy, metabolic intermediates, and protein for their replication cycle. In general, there are two kinds of cycles, one called the lytic cycle and the other the lysogenic cycle. Figures 2 and 3 depict two kinds of infection processes.

The lytic cycle is typically considered the main method of viral replication, since it results in the destruction of the infected cell. In this process, the first step of the lytic infection in its host cell is called attachment (adsorption). The bacteriophages adhere to the bacterial surface using their tail fibers by a chance collision at a chemically complementary site. After adsorption, the bacteriophage injects the DNA into the host cell through a process called penetration. In this process, the tail sheath contracts and the core inside the bacteriophage is driven through the wall to the membrane under mechanical and enzymatic conditions. Immediately after injection of the DNA, synthesis of early proteins, transcription, and translation of a section of the phage DNA begins. In the transcription process, the early proteins as the repair enzyme are produced in order to repair the broken bacterial cell wall. On the other hand, in the translation process, the DNase can degrade the host DNA into precursors of phage DNA; the phage-specific DNA polymerase will copy and replicate phage DNA. During this period, the final result is the synthesis of several copies of the phage DNA. The next step is called synthesis of late proteins. The replicated copies of phage DNA in the previous step can be used for is the synthesis of several copies of the phage DNA. The next step is called synthesis of

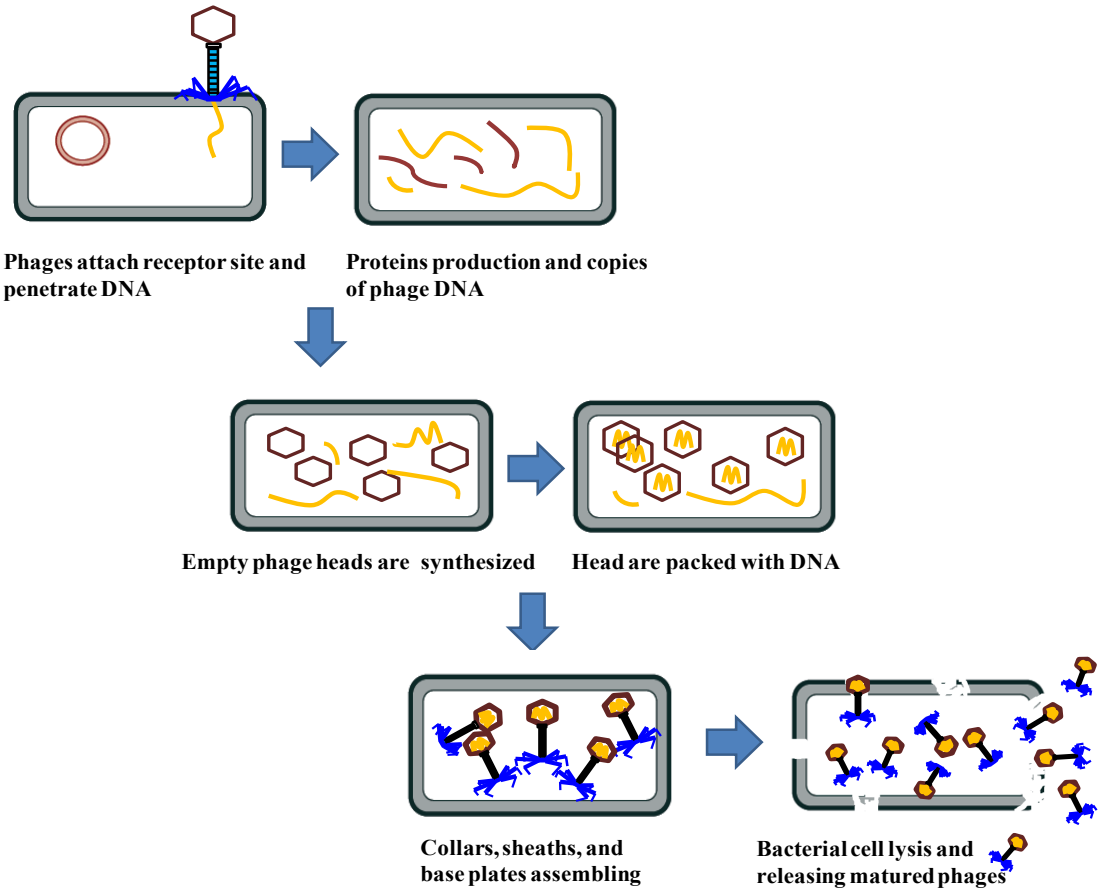

Figure 2: Lytic process of the bacteriophage infection process

late proteins. The replicated copies of phage DNA in the previous step can be used for transcription and translation of late proteins.

The structure of late protein is made up of capsomeres and the various components of the tail assembly. The lysozyme production is the last step of the replication process. It assembles in the tail and is used to escape from the host cell by breaking the cell wall. Thus, the host cell is lysed, releasing mature viruses.

Lysogenic cycle is another method of viral repro Lysogenic cycle is another method of viral reproduction. During the lysogenic cycle duction. During the lysogenic cycle

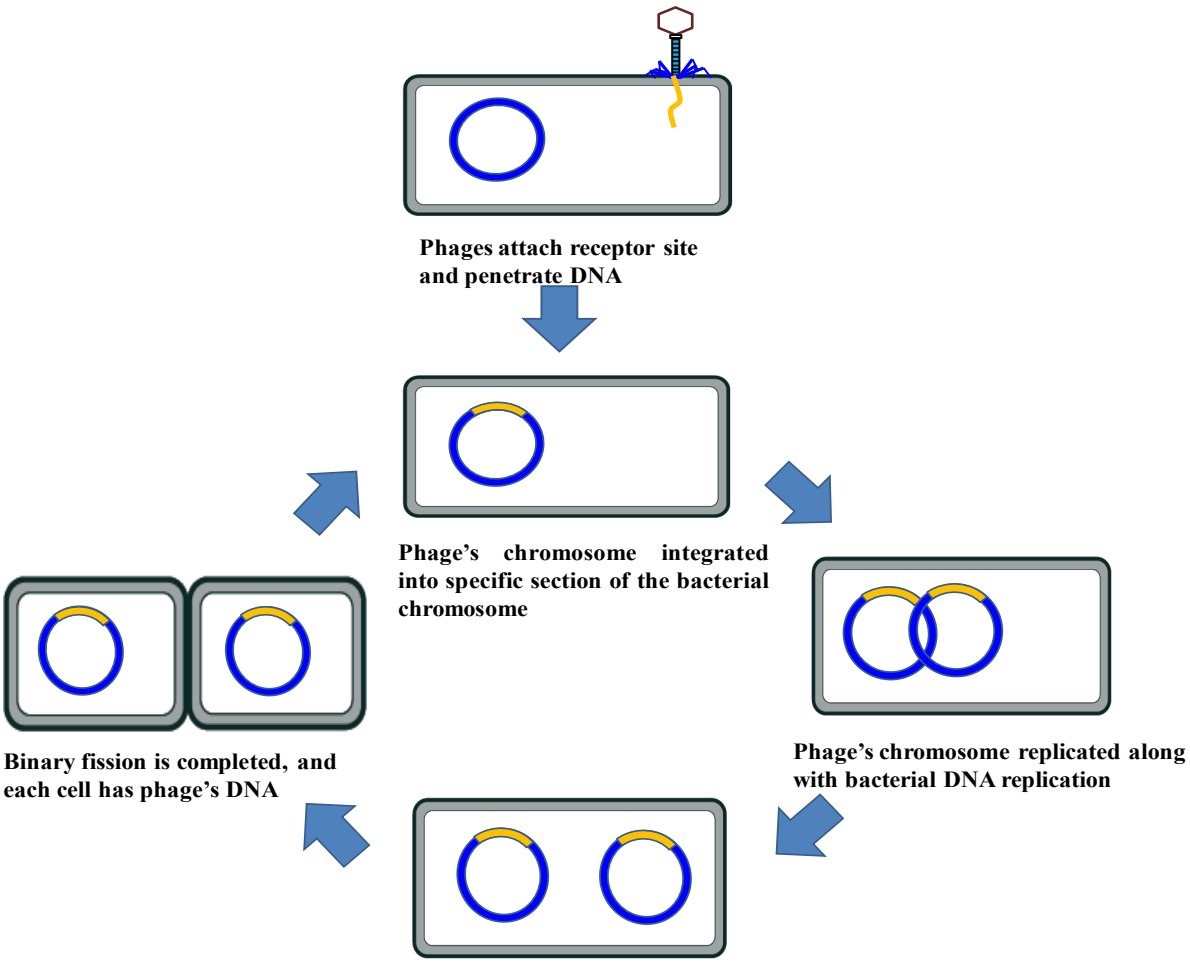

Figure 3: Lysogenic process of the bacteriophage infection process

process, bacteriophages' chromosomes will become integrated into a specific section(s) of the host bacterial cell instead of killing the bacteria. In addition, the phage genes can code for synthesis to prevent synthesis of phage enzymes and proteins required for the lytic cycle. This phage DNA is called prophage and the host bacteria are said to be lysogenized. These new integrated genetic materials can be transferred to each subsequent generation and released via a new lytic cycle caused by environmental stress (such as UV radiation or PH changing). This process is very rare; however, it also can

assure new phages are formed which can proceed to infect other cells. Bacteriophages are ubiquitous and are very important for freshwater and marine bacterial communities (Suttle 2006; Wommack and Colwell 2000). Bacteriophages have wide applications in environmental issues including controlling cyanobacterial blooms, and reducing the sludge bulking formation of filamentous bacteria.

1.5 Phage therapy for ARB biofilms

Phage therapy is the therapeutic use of bacteriophages to treat pathogenic bacterial infections. It is one approach that has great potential as a solution to the serious worldwide problem of drug-resistant bacteria (Parisien et al. 2008; Sulakvelidze 2005). While they were administered as antibacterial agents as early as 1919, before the discovery of antibiotics, inadequate understanding of phage biology and genetics reduced the efficacy of phage therapy (Gill and Hyman 2009).

When bacteriophages infect biofilms, the interactions will occur. The polysaccharide polymerase enzyme degrade the EPS and cause biofilm slough off and the biofilm's integrity might be destroyed, if the phage can produce polysaccharide-degrading enzymes. The interaction depends on the susceptibility of the biofilm cells to the phage and to the availability of receptor sites (Simoes 2010). It is known that fluorescent pseudomonas cells can be eliminated using bacteriophages and in the experiment, about 80% of biofilm was removed in the early stage of development and were 5 days old under optimal conditions (Sillankorva et al. 2004). In addition, there is some evidence that

indicates that bacteriophages can express biofilm-degrading enzymes which attack the bacterial cells in the biofilm and the biofilm matrix (Lu and Collins 2007).

There are two advantages of the phage therapy in biofilm reduction. The first one is that they can multiply in direct correlation to an available growing host; the second one is the bacteriophages' concentration will increase as long as its host is present in the enclosed environment. However, bacteriophages that infect cells at the surface will replicate, generating a high concentration of phage locally at the site of the infection, which can then progressively destroy the biofilm. In other words, bacteriophages can infect bacterial cells and destroy the newly revived cells continuously. In addition, bacteriophages can carry or induce the expression by the bacterial host of enzymes that dissolve the biofilm matrix (Pearl et al. 2008). One study shows that 84% of biofilms forming by *Pseudomonas fluorescens* strain were reduced by 10^9 PFU/ml of bacteriophages treated after 200 min and at 26□ (Sillankorva et al. 2008). In addition, another study indicated that 28-hour biofilm formed from *E.coli* 3000 was 6-log reduction after treating with 10^9-10^{10}PFU/ml phage.

One of the drawbacks of phage therapy is the narrow host range of bacteriophages. The phage receptors are different in gram-negative and gram-positive bacteria (Kutter et al. 2005), and therefore, some phages have specificity at the strain level. The diversity of bacterial infections implies that it may be difficult for any particular engineered phage to be a therapeutic solution for a wide range of biofilms. Because of the high specificity of phages, many negative results may have been obtained because of the failure to select

lytic phages for the targeted bacterial species. As a result, it is advantageous to design a phages cocktail, a mixture of phages with differing host ranges, which can degrade multiple extracellular polymers to cover a range of biofilm and target biofilms containing multiple strains or species.

All in all, this study focused on the single strain of *Chryseobacterium taeanense* K-2 biofilm development and the implications and performance of biocontrol based on bacteriophage. The results will be applied for modeling of biofilm systems researching for full-scale wastewater treatment facilities.

1.6 Objectives

The overarching goal of my research was to demonstrate the application of phage therapy for ARB biofilms. The following specific objectives accomplished my research goal.

Objective 1: Isolation and characterization of a model antibiotic resistant bacterium from wastewater.

Objective 2: Isolation and characterization of a lytic bacteriophage infecting the isolated ARB.

Objective 3: Demonstration of phage therapy for the isolated ARB biofilm.

CHAPTER 2

MATERIALS AND METHODS

2.1 Isolation and characterization of a model antibiotic-resistant bacterium from wastewater

2.1.1 Isolation of antibiotic-resistant bacteria (ARB)

The mixed liquor was collected from a local wastewater treatment plant and serially diluted in the ratio of 10^{-1}, 10^{-2}, 10^{-3}, 10^{-4}, and 10^{-5} using 0.85% (w/v) sterile saline solution. Subsequently, each diluted sample was plated uniformly onto the 2% modified R2A agar (Peptone 0.5g, Yeast Extract 0.25g, Agar 10g in 1 L deionized water) plate containing 40µg/ml kanamycin final concentration (Fisher Scientific, PA). The pH of the media was adjusted to 7.2 - 8.7. A method control was prepared in a similar way without antibiotic. The plates were then incubated at 37□ overnight.

Single isolated colonies were picked up and screened on antibiotic plates 4 times (subcultures) for obtaining pure culture of isolates. Purified subcultures were picked and grown in modified R2A medium (Peptone 0.5g, Yeast Extract 0.25g, in 1 L deionized water). Glycerol stocks of the pure culture were made from 12-h-old culture and store in -80°C until further use. Fresh liquid cultures of the isolate were made by inoculating a

glycerol stock in modified R2A medium each time.

2.1.2 Phylogenetic characterization of ARB using molecular tools

Genomic DNA from fresh 10 h culture was extracted using the Soil DNA extraction kit (MoBio Labs, Solana Beach, CA) following manufacturer's protocol and extracted DNA was verified on a 1 %(w/v) agarose gel. PCR amplication of 16S rRNA gene was performed using universal primer, 8f (5'-AGAGTTTGATCMTGGCTCAG-3') and reverse universal primer, 1492r (5'-GGYTACCTTGTTACGACTT-3'), 2X GoTaq Mastermix and genomic DNA as a template. PCR program: initial denaturation at 95ºC for 5 min, 30 cycles of 90 sec denaturation at 95ºC, 120 sec of annealing at 52 ºC, and 3 min of extension at 72 ºC, with a final 10 min extension at 72º was used. Amplicon obtained from PCR was verified on 1 %(w/v) agarose gel and purified using a gel extraction kit (Qiagen, CA). The purified amplicon was sequenced using universal 8f and 1492r primers on an ABI PRISM 377 automated DNA sequencer (Applied Biosystems, USA). The sequences obtained were analyzed for homology using a web-programs BLAST and seqmatch. MEGA version 5 (http://www.megasoftware.net/) was used to align the sequences and generate the phylogenetic tree.

2.1.3 Biochemical characterization of isolated ARB using Gram staining

Gram staining is widely used to distinguish two large groups of bacteria based on different cell wall constituents. The Gram positive bacteria stain violet due to the presence of more peptidoglycan in their cell walls which can retain the crystal violet.

Gram negative bacteria stain pink (by secondary stain-saffranin), because of their thinner peptidoglycan wall which cannot retain the primary stain, crystal violet.

First, bacteria (from 10 h old fresh culture) was mounted onto a clean glass slide using a sterile inoculation loop and heat-fixed. The slide is then flooded with primary stain Crystal Violet for 1 min, following which the mordent, Gram's Iodine, was added. After 1 min, the excess stain was drained and slides were rinsed with deionized water. Slides were then decolorized with 100% ethanol for 1 min and rinsed with deionized water. Sunsequently, the slides were treated with secondary counter stain, safranin.

2.1.4 DAPI (4', 6-diamidino-2-phenylindole) staining analysis

DAPI (4', 6-diamidino-2-phenylindole) is a fluorescent stain which is used extensively in fluorescence microscopy because it binds strongly with DNA. Fresh 10 h old bacterial culture was diluted 20 times in 1X Phosphate Buffer Saline (PBS), and fixed for 20 min in 4% paraformaldehyde. The fixed cells were collected on 0.22 µm polycarbonate membrane filter (GE Water & Process Technologies). Cells collected on the filter paper were carefully transfered on a clean microscope slide (Fisher Scientific). The cells on the slide were stained with 100 µL of 5µg/mL DAPI solutiuon and incubated in the dark for 20 minutes. The slides were then washed with sterile deinoized water a few times, and air dried for 5 min. A clean cover slide was put onto the microscope slide after the antifade solution was added on the sample and sealed with nail polish. The slides were then viewed under the appropriate filter of an epifluorescent microscope (Olympus

BX51).

2.1.5 Growth curve

In microbiology, growth is defined as an increase in the number of cells. Microbial cells have a finite life span, and a species is maintained only as a result of continued growth of its population. A viable count measures the cells in the culture that are capable of reproducing. Optical density (turbidity), a quantitative measure of light scattering by a liquid culture, increases with the increase in cell number (Madigan et al. 2010). To determine the growth of *C. taeanense K-2,* 100ml of log-phage culture was inoculated into 1 L R2A medium and incubated at 37□ with agitation provided. An aliquot of 1ml bacterial culture was collected at an interval of 30 min and the optical density of the culture was measured at 600nm. Sterile R2A media was used as blank. Growth-curve was deduced by plotting OD vs time (Sigmaplot).

2.2: Isolation and characterization of a lytic bacteriophage infecting the isolated ARB

2.2.1 Isolation of lytic bacteriophage

The principle for determination of infection of the host bacterium by a bacteriophage is based on the single phage infecting the host, multiplying, and releasing their progeny, resulting in host cell lysis. The continuous infection causes the host cell lysis on agar plates. This process can be achieved by the double layer agar technique. The double layer agar technique is also known as the “soft agar overlay,” or “top-agar” method of

plaque assay (Walker et al. 2009). The plaques appear on the 1% top agar after overnight incubation. The bacteriophage and the bacteria host are mixed with 1% top agar and spread on the base agar plate. The bacteriophage progeny will inhibit the host growth and result in the formation of clear zone (Figure 4). As shown in the figure, clear and turbid (cloudy) plaques may appear, representing lysogenic and lytic phage infection, respectively. Mixed liquor from the local full-scale wastewater treatment plant were obtained. In order to remove suspended particles and microorganisms, the mixed liquor sample was filtrated through 0.45 and 0.22 μm filters (Millipore, CA). The bacteriophages present in the filtrate were concentrated using Amicon Ultra-4 with MWCO 30000 (Millipore, CA). The concentrate obtained from the above centrifugation was used as phage stock in the subsequent studies.

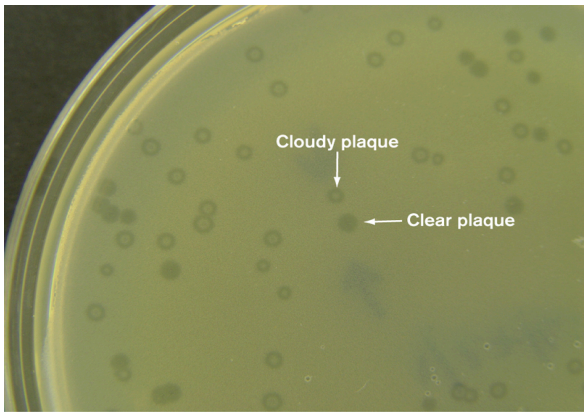

Figure 4: Cloudy plaque and clear plaque.
[http://www.wwnorton.com/college/biology/microbiology2/ch/10/etopics.aspx]

From a fresh 10 h *C. taeanense* culture, 1ml aliquot was infected with 1µl of the above phage stock, mixed thoroughly on a vortex mixer and incubated at room temperature for 15-30 min. To this, 3ml presterilized molten 1% top agar (10g bacto-agar, 1g peptone, 0.5g yeast extract in 1L deionized water) was added and mixed thoroughly on a vortex mixer. The mixture was then spread on a premade 2% base agar plate. A negative control was prepared using the similar protocol without adding the phage stock. The plates were incubated at 37°C overnight. The plates that showed clear plaques were selected to make the lysate stock. These plaques were then picked using a sterilized pasture glass pipette, after which, the plaque with agar was transferred into a fresh and sterile polypropylene tube and resuspended in the SMG buffer (5.8 g NaCl, 2.46 g $MgSO_4$, 7.9 g Tris-HCl, 0.1 g Gelatin in 1L deionized water). The phage solution in SM buffer was stored at 4°C until further use. The isolated phage-stocks were screened using the repeated subculture method to obtain a pure phage-stock.

2.2.2 Viral enumeration using epifluorescence microscopy (EFM)

To indentify and enumerate the virus-like particles existing in the phage stock, the bacteriophage samples were filtered through 0.22 µm filter (Millipore,CA) to remove the suspended solids. In order to exclude the free bacterial DNA, 900 µL of the above filtrate was added to 100 µL of RQ1 reaction buffer and 2 µL of RNase free DNase I (Invitrogen) in a fresh polypropylene tube. After incubation for 20 min at 37 □, 35 µL of 0.5 M EDTA was used to stop the DNase activity. The DNase treated sample was

vacuum filtered through a stack of 25mm filters consisting of 0.02 µm Anodisc (Whatman Int'l Ltd., Maidstone, England), a 0.22 µm Durapore membrane filters (Millipore, CA), and a glass fiber prefilter (Millipore, CA). Virus-like particles (VLPs) collected on the Anodisc filter were stained using 4 µl SYBR Gold stain 800 µl SMbuffer for 20 min. Finally, the Anodisc filter was transferred onto the slide containing a drop of freshly prepared antifade solution (Kotay et al. 2010) and sealed with a clean cover glass. The slides were observed under an Olympus BX 51 epifluorescence microscope (Olympus, Japan) using a Cy3 filter and VLPs were enumerated using the micrographs captured.

2.2.3 Characterization of the isolated phage

The phage titer defines the concentration of infectious viral particles per milliliter of growth medium. By counting the number of plaques and multiplying by the serial dilution factor, we can determine the titer, which is the concentration of phage in the phage stock. To determine the titer, the phage stock was serial diluted 10^{-1}, 10^{-2}, 10^{-3}, 10^{-4}, 10^{-5}, 10^{-6} times using sterile prefiltered SMG buffer. From each dilution of phage stock, 1µl was added into 1 ml of fresh 10 h *C. taeanense K-2* culture and incubated at room-temperature for 1 h. To the mixture, 3ml 1% top agar was added, mixed thoroughly, and poured onto 2% base agar plates. Triplicates of each dilution were plated and plates were incubated at 37°C overnight.

CsCl density gradient method was used to purify the phage. First, 2 ml of cesium chloride with a density (ρ) of 1.6g/l was added into the bottom of an ultracentrifuge tube (Beckman, CA). On top of that, 2 ml of 1.4 g/l of cesium chloride was carefully overlaid using a syringe. On top of that, 2 ml 10% sucrose and 4 ml of sample were carefully overlaid without disturbing the layers below. Samples were centrifuged, at 36,000 rpm, at 20 °C for 2-3 h. The purified phage appeared as a distinct band at the interface of the ρ=1.4 g/l layer and ρ=1.6 g/l layer. The phage band was carefully siphoned from the side of the tube by using a syringe, transferred into a clean dialysis tube (Fisherbrand) and dialyzed overnight in SMG buffer to remove the CsCl and extra ions.

On a clean 400 formvar-coated copper grid (Fisherbrand), 3.5 uL of the CsCl purified phage was loaded and incubated at room temperature for 2 mins. The excess liquid was soaked from the side of the grid using bibulous paper (Fisherbrand), and the sample was stained using 2 mL 1% uranyl acetate for 2 min (Kotay et al. 2010). The grids were observed under a Tecnai T12 Transition Electron Microscope (FEI, Japan). An accelerating voltage of 80 kV was used and micrographs revealing bacteriophage morphology were recorded.

2.2.4 Live and dead bacterial enumeration (EFM)

Live/Dead BacLight™ (Molecular Probes Inc., CA) staining is one of the most important fluorescence assays used to determine and mark living bacteria. The major advantage of this method is it is easy to classify bacterial cells as living or dead in a few

minutes. There are two kinds of stains, green fluorescent SYTO® 9 and red fluorescent propidium iodide nucleic acid stains. These stains have the ability to label live and dead bacterial cells due to the diversity of their spectral characteristics. During the staining processing, the SYTO® 9 could stain both live and dead bacteria cells. The propidium iodide was just able to label live bacterial cells due to the ability of penetrating damage of the bacterial cell membrane and displacing SYTO® 9 fluorescence. The emission maxima of the SYTO® 9 and propidium iodide nucleic acid are 480 nm/500 nm and 480 nm/625 nm. Therefore, live and dead bacteria can be viewed separately or simultaneously by fluorescence microscopy with suitable optical filter sets.

A BacLight bacterial viability kit has been used to determine the live and dead numbers of bacterial cells. *C. taeanense* was inoculated in a 10 ml R2A medium for 8 to 10 h and a 1 ml culture was filtered through 0.22 μm membrane filter (Millipore Inc.). After that, the bacteria captured on the filter were stained with a BacLight bacterial viability kit (Molecular Probes Inc.) in the dark for 20 min. The filter was fixed on the glass slide and sealed well and was analyzed by using a BX 51 microscope (Olympus, Japan) with Cy3 and a FITC filters to capture the micrographs. Finally, the numbers of the live and dead cells were calculated from the micrographs using ImageJ.

2.2.5 Phage-to-host ratio analysis

Phage-to-host ratio (PHR) is a critical parameter which is an index of infectivity of the bacteriophage towards the host bacterium. To determine the optimal PHR, 1:1, 10:1,

10^2:1, 10^3:1, and 10^4:1 ratios of bacteriophages to the host, *C. taeanense K-2,* were initiated. Following 9 h of infection, the cultures were tested for final O.D., Bacteria Live/Dead ratio, and VLPs enumerated. A negative control without bacteriophage was also tested along with the above samples.

2.2.6 One-step growth curve

In order to determine and construct the one-step growth curve of the *Chryseobacterium taeanense* bacteriophage, 1 mL of *Chryseobacterium taeanense* culture, with a population of 10^5, was transfered into the sterile polypropylene tubes and each sample in triplicate. Subsequently, 3×10^6 plaque forming units (PFU) of the isolated bacteriophage solution was added into each tube and incubated at 37 ℃ for 1 min, after which, the pallet was resuspended in a fresh R2A medium after being centrifuged by 6000g for 1 min at 4 ℃. Next, the resuspended pallet was added to the 1 L *Chryseobacterium* culture which was growing in the log growth phase. The *chryseobacterium* culture contained bacteriophages that were incubated at 37 □ with starring and 1 ml infected culture was taken to test the PFU each 10 min. Each subsample from the set of triplicate samples at each time interval was divided into two equal halves, of which, one half was used to calculate the total PFU (free phage plus any infectious intracellular phage particles) after adding the chloroform and the other half was used to calculate the free PFU (extracellular/nonadsorbed). The counts obtained from triplicate values were averaged and were plotted to obtain the one-step growth curve (Ellis and

Delbrűck 1939). The burst size was calculated by dividing the number of virus-like particles released from the cell with the number of virus particles initially added.

2.3 Biofilm quantification and analysis

2.3.1 Biofilms formation and phage therapy

The biofilms were formed on the glass slide which was inoculated into 5-slidesmailer (Fish scientific Inc.). After inoculation of 16, 54, and 84 days, the glass slides were divided into two parts, one without phage infection, the other part infected by phages. The phage titer of 10^{13} of phage solution was used to infect the biofilm overnight. Live and dead bacterial cell analysis was done using a Baclight bacterial viability kit and (Molecular Probes Inc.). In addition, the EPS of the biofilm was stained with Calcoflour White (ENG Scientific, Inc).

2.3.2 Biofilms quantification using epifluorescence microscopy

The biofilms with the dye mixture were incubated in the dark for 30 min and were analyzed using a BX 51 microscope (Olympus, Japan) using Cy3, Cy4, and FITC filters to capture Live/dead cells and EPS, respectively. At each parameter tested, multiple pictures were overlayed and captured to quantify the percentages of Live/dead cells and EPS using BioImageL. For biofilm image quantification, the cell accounting program of the BiomageL will enumerate the total bacterial biomass and calculate distribution of the green and red biomass. The biomass identified as other colors will be labeled as ‘Not Segmented’ (NS).

2.3.3 Scanning electron microscope images analysis

The scanning electron microscope (SEM) uses a high-energy electron beam to generate a signal at the surface of solid specimens. A scanning electron microscope can receive signals from the electron sample and collect data from selected areas of the surface of the sample. Then a 2-dimensional image is created that displays spatial variations in these properties. The range of areas from 1 cm to 5 microns in width can be imaged in a scanning mode using conventional SEM techniques (magnification ranging from 20X to approximately 30,000X, spatial resolution of 50 to 100 nm). Also, SEM can do the point locations analysis, such as chemical compositions, crystalline structure, or surface texture determination.

Compared with traditional microscopes, scanning electron microscopes have many advantages. SEM has a larger depth of field and higher resolution, which allows the specimens to be magnified at higher levels. SEM use electromagnets instead of lenses. Therefore, it has a larger degree of magnification. All in all, based on these advantages, the scanning electron microscope becomes one of the most useful instruments in the image analysis researching field.

First, the glass slides with incubated biofilms were divided into two parts; one is the control part without phage infection, the other part infected with phages overnight. Then, the slides were fixed using an EM solution (1% paraformadehyde and 2.5% glutaraldehyde). The biofilms on the slide were washed with 0.1 M cacodylate buffer (Ted Pella Inc., USA) twice for 5 min. Then, the slides were treated for 45 min with

postfix solution (2% OsO_4 in 0.1 M cacodylate buffer). Subsequently, the biofilm was dehydrated in a gradient of (50% - 70% - 90 % -95% - absolute) alcohol solution and dried using hexamethyl disilazane (3 treatments). The slides were left overnight and Gold coated for 15 -30 sec, using 108□ Sputter Coater (Ted Pella Inc., USA). Finally, the slides were analyzed in a Hitachi S-2460N scanning electron microscope and micrographs were taken at 20kV.

CHAPTER 3

RESULTS AND DISCUSSION

3.1 Characterization of *Chryseobacterium taeanense k-2*

3.1.1 Isolation of antibiotic-resistant bacterium, *Chryseobacterium taeanense k-2*

Antibiotic-resistant bacterium, *Chryseobacterium taeanense K-2,* was isolated from the mixed liquor of a local full-scale wastewater treatment plant in the presence of kanamycin (40μg/ml final concentration). Three distinct bacterial colonies based on differentiation of color appeared on kanamycin-spiked R2A agar plates. *C. taeanense k-2* formed visible yellowish colonies 2-3 mm in diameter with clear and entire circular edges after incubation for 16-24 h at 37°C (Figure 5). Pure culture of *C. taeanense k-2* was obtained following repeated subculture of isolated colonies using the streak-plate method. *C. taeanense k-2* was found to grow in the presence of kanamycin both on agar plates and liquid R2A media. The other two isolated colonies of antibiotic-resistant bacteria were investigated in a parallel research (by graduate students).

It is not surprising that antibiotic-resistant bacteria were found in water samples from many U.S. municipal wastewater treatment plants, because bacteria that are resistant to chemically modified and synthesized antibiotics are widespread in the environment, as

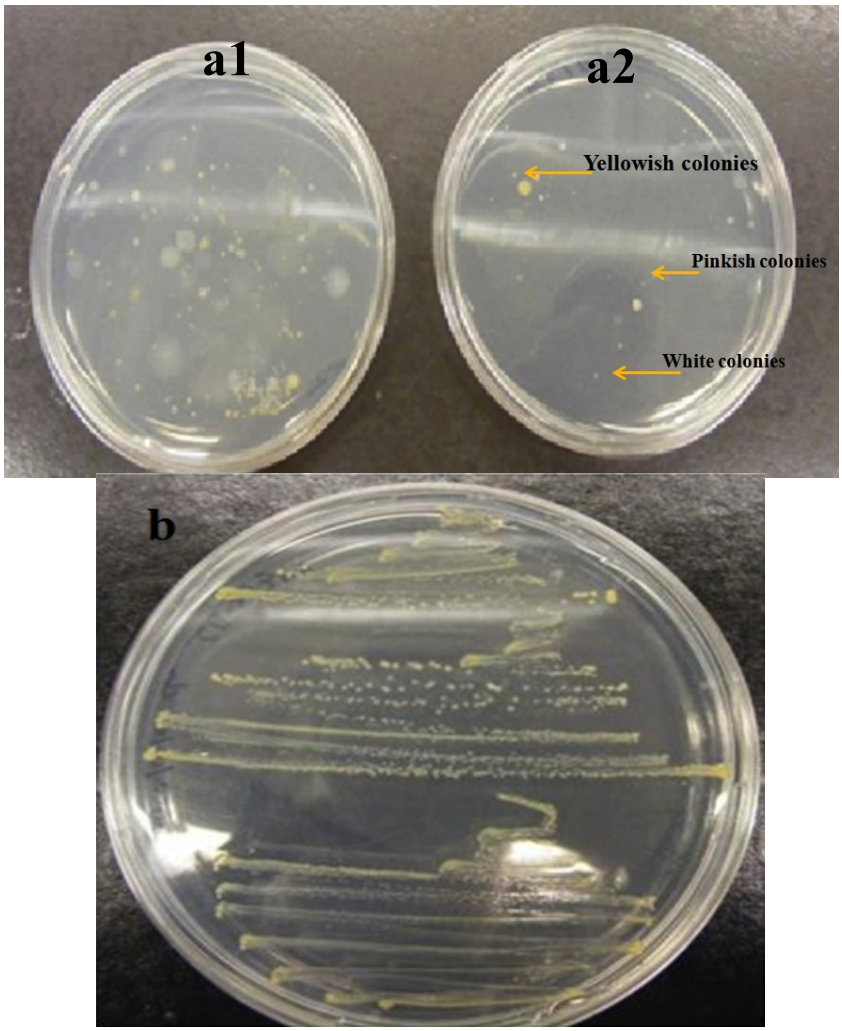

Figure 5. Agar plates (a1) without (a2) with Kanamycin (40 µg/ml) depicting isolated colonies (b) purified streaked subculture of *Chryseobacterium taeanense K-2*.

revealed in previous studies (Ash et al. 2002). Most studies, however, were focused on screening for established antibiotic-resistant pathogens with a clinical perspective.

This study, on the contrary, focused on random and unconventional bacteria that were resistant to antibiotics. The intention was to investigate the prevalence of antibiotic resistance among uncommon bacteria and natural flora of wastewater treatment systems.

Limitations of this study were: i) a culture-based method was used to screen

antibiotic-resistant bacteria and it is necessary to note that most bacteria in nature cannot be cultivated; ii) kanamycin was the only antibiotic used for screening, however, wastewaters are expected to harbor much more diverse bacteria that could be resistant to much more potent antibiotics.

3.1.2 16S rRNA gene phylogenetic analysis

Determination of evolutionary relationships between organisms can be inferred by comparing the nucleotide or amino acid sequence. Smaller subunit ribosomal RNA (rRNA)-based fingerprinting is a well-established molecular tool to discern taxonomic affiliation and evolutionary relationships in prokaryotes. Carl Woese was the first microbiologist to use rRNA sequence analysis as a measure of microbial phylogeny and revolutionize our understanding of cellular evolution. The divergences among the microorganisms are depicted in the form of a phylogenetic tree using a treeing algorithm.

A complete sequence of 16S rRNA (1390bp long) of the isolated antibiotic-resistant bacterium obtained from the sequencing was analyzed for homology match on BLAST (NCBI). The BLAST revealed 99% maximum identity and 99% coverage with *Chryseobacterium taeanense* strain NBRC 100863 (NCBI Accession # AB681269) and strain PHA3-4 (NCBI Accession # NR_043254).

To our knowledge, there is no pathogenecity or antibiotic resistance attributed to the strains *Chryseobacterium taeanense;* however, other species belonging to the genera *Chryseobacterium* have been reported which cause infections in humans. Since the

bacterium isolated in the present study was the second of the three colonies isolated on the kanamycin plate, it was named *Chryseobacterium taeanense* strain K-2. *C taeanense* belongs to the family *Flavobacteriaceae* under the phylum *Bacteroidetes* as retrieved from the (NCBI) taxonomy database.

The phylogenetic tree based on the 16S-rRNA gene sequences was populated using the maximum likelihood algorithm in MEGA version 5.0. Evolutionary distance matrices for the maximum likelihood method were generated according to the Tamura-Nei distance model. The resultant maximum likelihood tree topology was evaluated by bootstrap analysis based on 5000 resample datasets. The analysis substitution type used was "Nucleotide". Phylogenetic affiliation of *Chryseobacterium taeanense* strain K-2 towards other species in the genus of *Chryseobacterium*, and other *Flavobacteria*, was evident from the lineage that appeared in the phylogram (Figure 6). Among the eight *Chryseobacterium* species presented, *Chryseobacterium taeanense* strain PHA3-4 was the closest neighbor sharing 99% gene sequence similarity.

3.1.3 Growth analysis of *Chryseobacterium taeanense K-2*

For testing and describing the bacteria growth curve, it is necessary to determine the number of cells representative of each single sample in different individual periods, because it is not easy to measure the culture's accurate cell number. Therefore, optical density (Absorbance @600nm) profile and plate count method via enumeration of Colony Forming Units (CFUs) was employed to deduce the growth curve of the

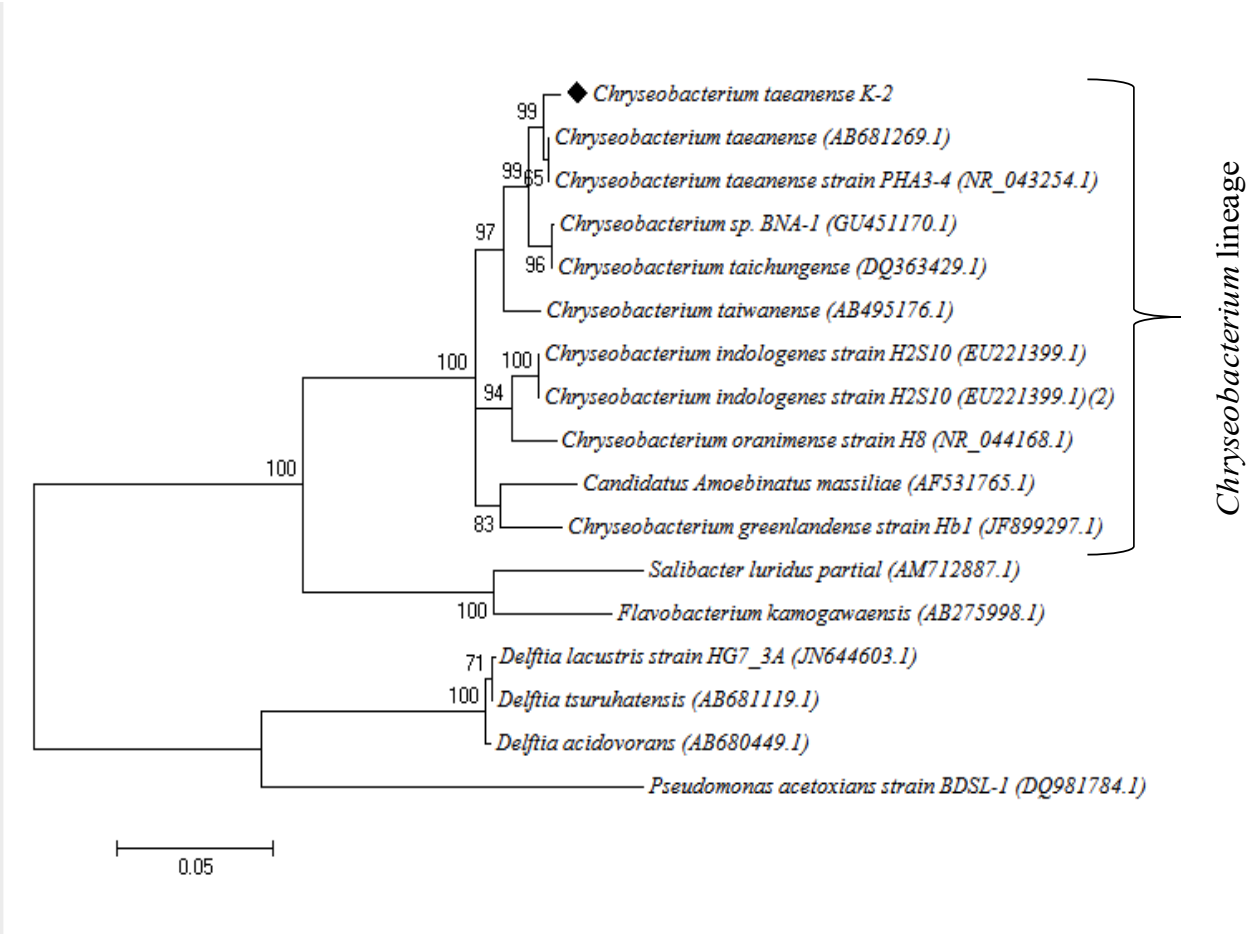

Figure 6. Phylogram depicting the phylogenetic relationship of *Chryseobacterium taeanense K-2*

bacterium (Figure 7a and b). There was no lag phase recorded in the growth profile as the inoculum used was actively dividing cells grown in the same nutrient media. The exponential (log) phage was around 10 h long, after which the stationary phase appeared. As deduced from the growth curve, the culture's cell population doubling time is 2.21 h and the maximum specific growth rate of *Chryseobacterium taeanense K-2* was around 0.022/h (Figure 7c).

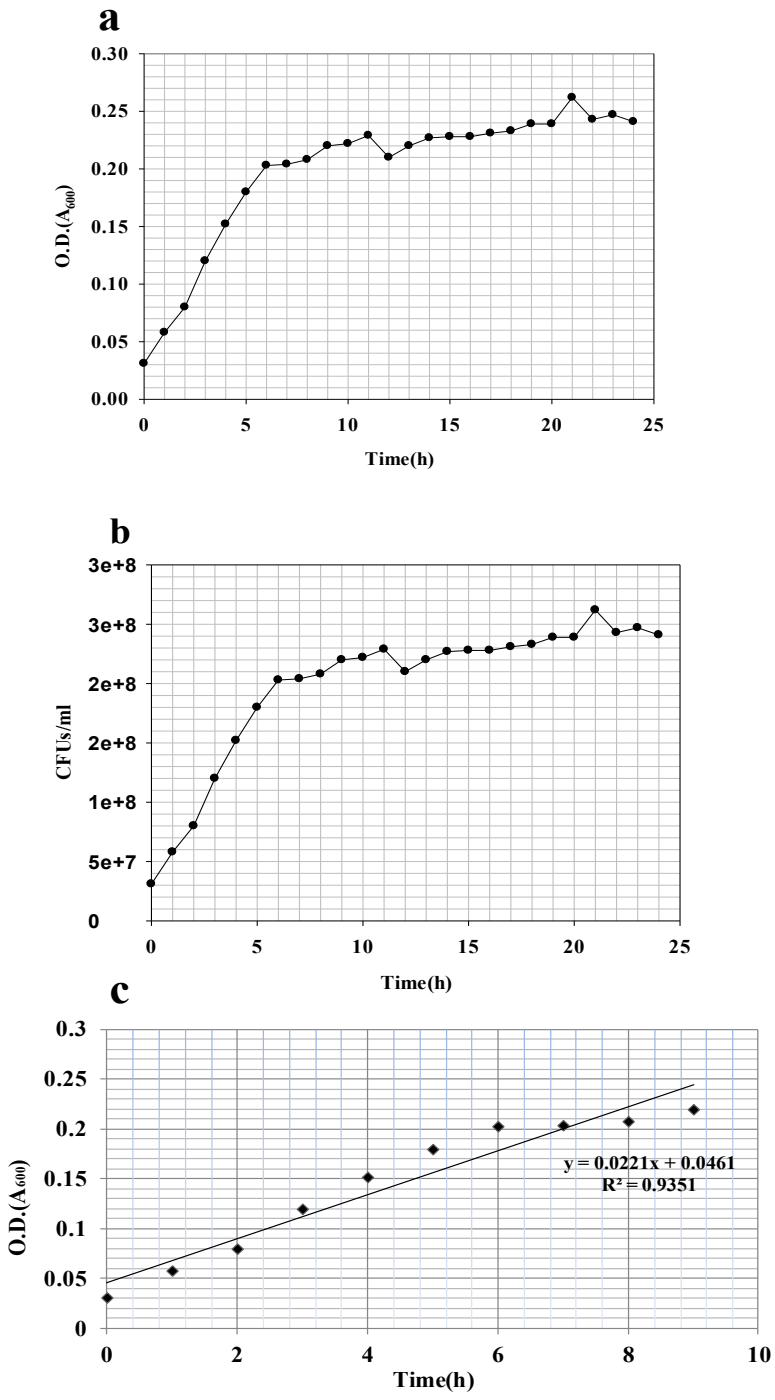

Figure 7. Growth curve of *Chryseobacterium taeanense K-2* obtained based on a) Optical density and b) Plate count method; c) depicts maximum specific growth rate

3.1.4 DAPI (4',6-diamidino-2-phenylindole) staining analysis

DAPI binds strongly to the A-T rich region on the DNA and is therefore used extensively in fluorescence microscopy. DAPI can pass through an intact cell membrane; therefore, it can be used to stain both live and fixed cells, though it passes through the membrane less efficiently in live cells and therefore, the effectiveness of the stain is lower. DAPI staining reveals that the morphology of the *Chryseobacterium taeanense K-2* is coccoid 0.5-1.0 μm cell-length (Figure 8) Myung et al. (2006) reported similar morphology of *Chryseobacterium taeanense*.

3.1.5 Gram staining

During the staining process, the Crystal Violet (hexamethyl-para-rosaniline chloride) interacts with aqueous KI-I2 via a simple anion exchange to produce a chemical precipitate (Brock et al. 2004). The Gram-positive bacterial cell wall has more lipids than Gram-negative bacterial cell walls. Thus, during the distaining process, alcohol will dissolve the lipids presence in the membrane and cell wall. While the Gram-negative bacteria cell has thinner peptidoglycan, it does not have enough ability to retain dye-iodine. Hence, Gram-negative bacterial cells readily get decolorized. Moreover, the Gram-positive cells will dehydrate and the cell wall will shrink by ethanol treatment. Therefore, the dye iodine complex will stay inside the thick peptidoglycan layer and does not get decolorized. It is easy to narrow the scope of the bacteria to identify the isolated

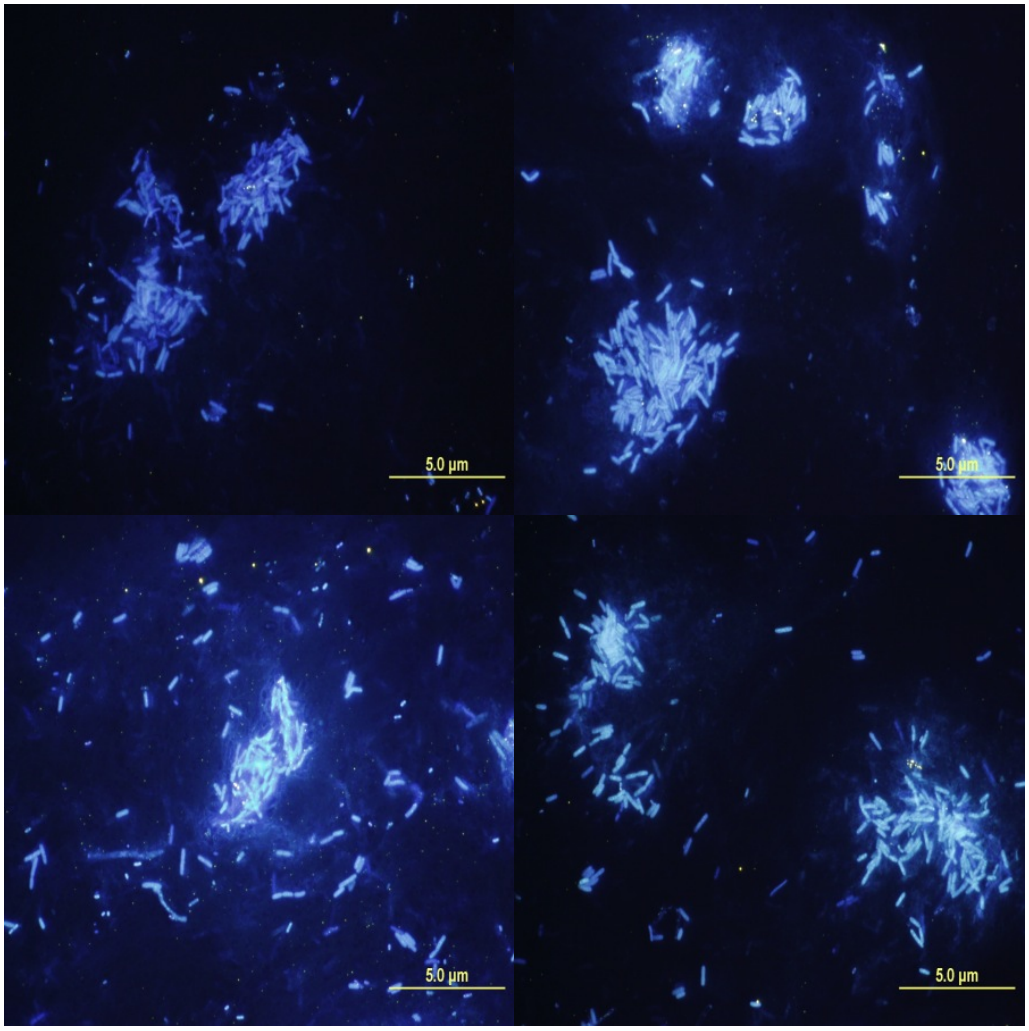

Figure 8. Micrographs obtained from DAPI analysis of *Chryseobacterium taeanense K-2* from the log-phage culture.

bacteria by Gram staining. Moreover, Gram reactivity can be used as a reference for the use of antibiotics in the medical field.

In this study, the Gram staining analysis inferred that the *Chryseobacterium taeanense K-2* was Gram-negative. Phase-contrast micrographs (Figure 9) confirmed the morphology (0.1-0.5 µm coccoid) revealed through DAPI staining of *Chryseobacterium taeanense*.

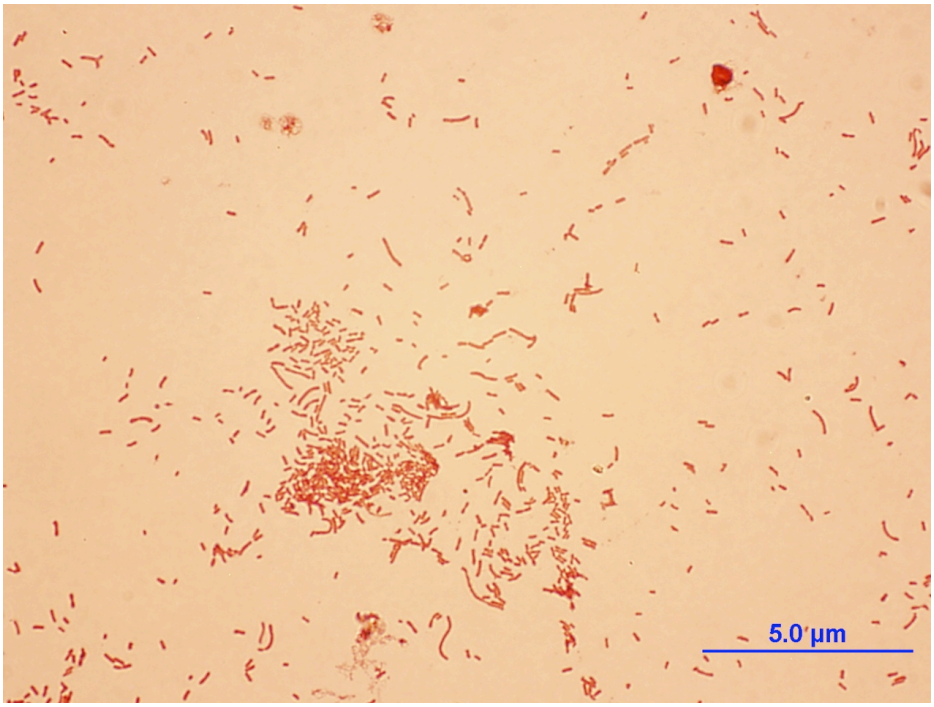

Figure 9. Phase-contrast micrographs of Gram-negatively stained *Chryseobacterium taeanense k-2*

3.2 Characterization of bacteriophage of the host of *Chryseobacterium taeanense K-2*

3.2.1 Isolation of bacteriophage

Lytic bacteriophages specific to *Chryseobacterium taeanense K-2* were successfully isolated from the mixed liquor sample obtained from the full-scale wastewater treatment plant (Central Valley Water Reclamation Facility-CVWRF). The repeated plaque assay technique produced clear plaques that were visible on 1% top agar when concentration phage-stock was used. This finding clearly implies that the possibility of finding a lytic phage infecting a host bacterium from the same habitat is significantly higher. The agar plate (Figure 10) contained several clear plaques instead of cloudy or bull-eyed plaques (Ellis, and Delbru¨ ck, 1939; Uchiyama et al. 2009) obtained after serial infection of *Chryseobacterium taeanense* K-2, suggesting the plaques were formed by lytic but NOT lysogenic phages. Three distinct plaques based on size of plaques viz. CTP-1 (0.5-1mm diameter), CTP-2 (0.1-0.2 mm diameter), and CTP-3 (0.1-0.2 mm diameter) were chosen for subsequent screen. Repeated plaque assay found that CTP-3 can have consistent infectivity and a significantly higher rate of infection. Therefore, CTP-3 was chosen for further study.

3.2.2 Viral enumeration using epifluorescence microscopy (EFM)

Figure 11 is the epifluorescent micrograph showing the distribution of Virus–Like-Particles (VLPs) present in the phage-stock of the lytic bacteriophage. The

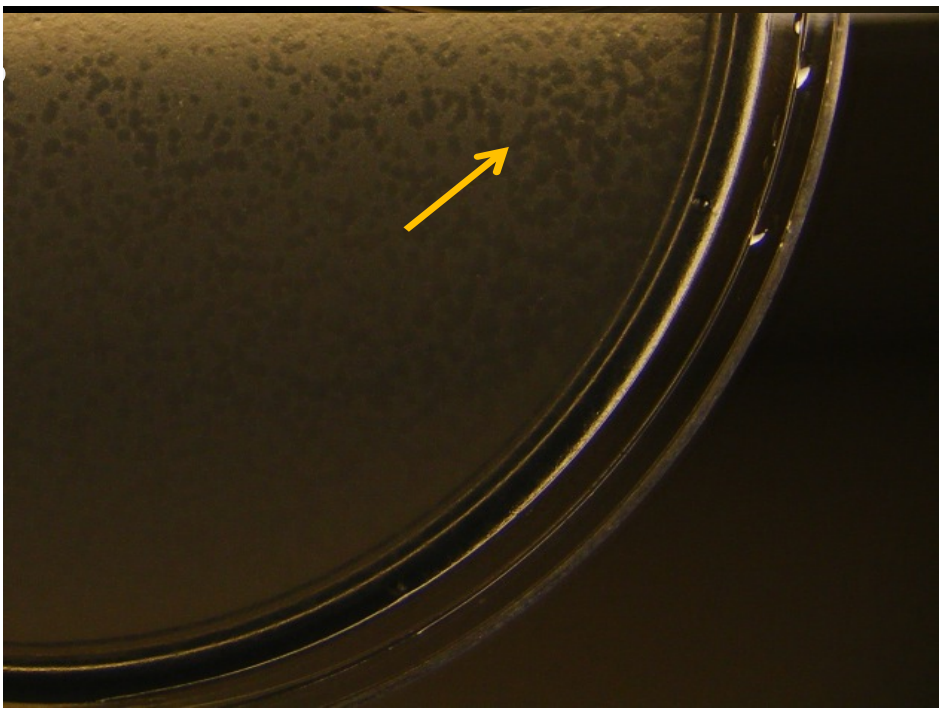

Figure 10. Agar plate containing clear plaques.

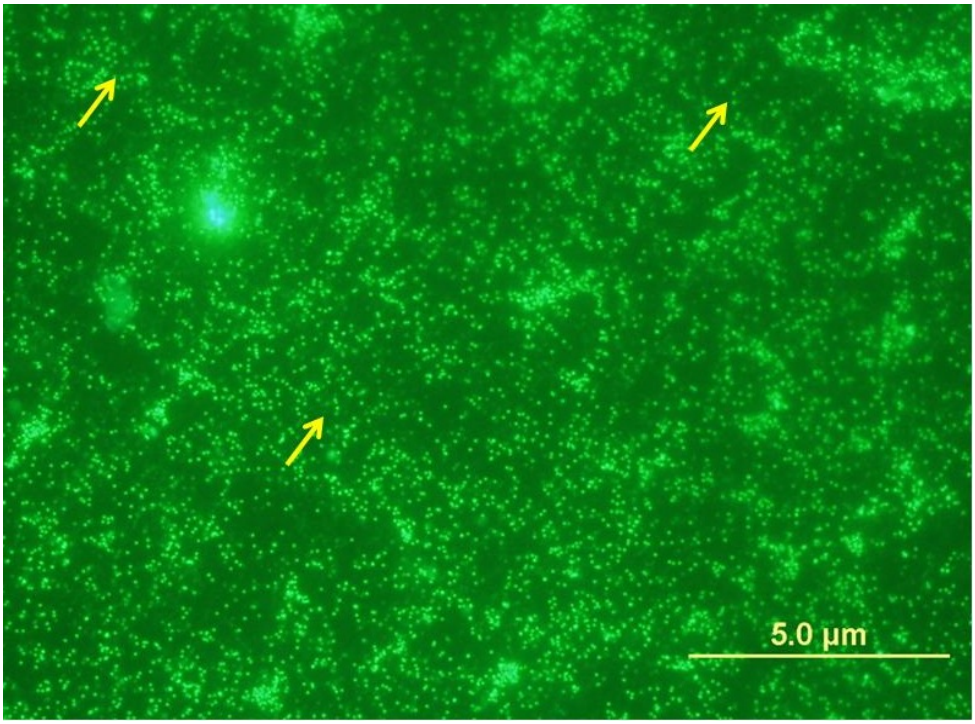

Figure 11. Virus-like particles (green dots) pointed by yellow arrows in the epifluorescent micrographs.

yellow arrow in the figure points to the VLPs (distinct green dots), suspended in the phage-stock stained with SYBR Gold. The titer of the *Chryseobacterium taeanense K-2* phage-stock obtained from progressive infection was calculated to be 1.11E+14 PFU/mL. EFM micrographs can provide a synoptic picture of Virus-like particles for their quantification, distribution, and abundance in a given samples. Due to the existence of single-stranded DNA or RNA viruses (which do not bind nucleic acid stains), it is not always accurate to estimate the abundance of virus using EFM. Furthermore, environmental samples may contain particles which can nonspecifically bind these nucleic-acid stains, resulting in false-positive enumeration. Therefore, direct plating plaque assay in associated with TEM-based and EFM-based VLP enumeration is recommended for the quantification of the virus. Despite these limitations, EFM-based technique can provide a rapid snapshot of VLP number in a sample.

3.2.3 Purification of lytic bacteriophage

CsCl density gradient centrifugation of the phage-stock obtained from a smaller infection volume did not result in a visible band of purified virus at the interface of 1.4g/l and 1.6g/l CsCl. Therefore, a progressive infection of *Chryseobacterium taeanense* K-2 with the phage-stock using a final volume of 1L 10 h old culture was used. Following overnight centrifugation, the viral pellet resuspended in the SMG buffer was used for CsCl density gradient centrifugation which revealed a distinct band (Figure 12). Purified phage-stock obtained after the dialysis of this band was used for TEM analysis.

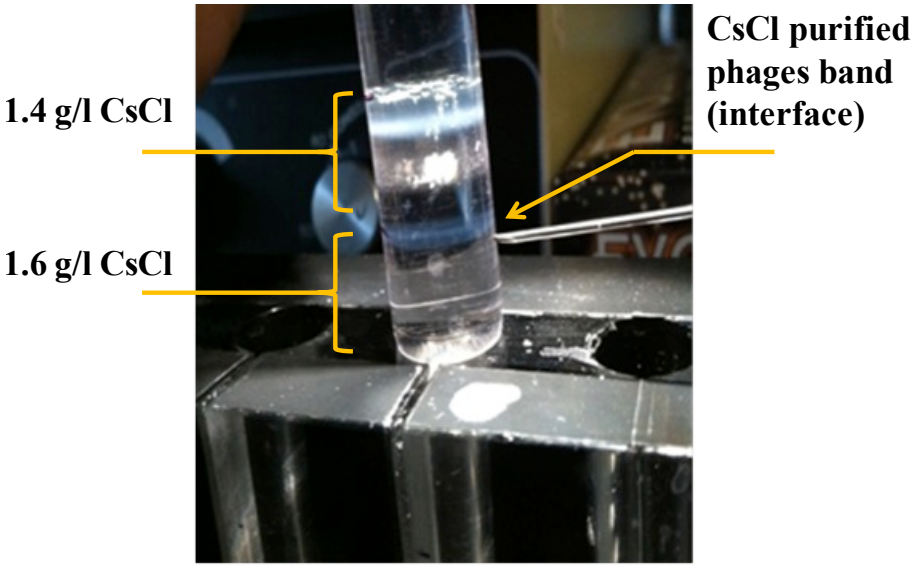

Figure 12. The bacteriophages' band after Cesium chloride density gradient purification

3.2.4 Transmission electron microscopy (TEM) analysis

TEM analysis shows that the isolated lytic bacteriophages infecting *Chryseobacterium taeanense K-2* have icosahedral geometry (Figure 13). The lytic bacteriophage had a very short noncontractile tail and a hexagonal head. The total length of the phage ranged from 90 to 100 nm. The diameter of the hexagonal head was 85 nm. The tail is noncontractile without subterminal fibers. The maximum length is ~23 nm. Table 1 enlists the multiple dimensions of the phages recorded in the TEM micrograhs. Based on the morphology revealed by the TEM-micrographs (Figure 13 a and b), the isolated bacteriophages belong to the Podoviridae family. These viruses have been reported to be lytic phages rather than lysogenic. Some TEM micrographs also showed ellipsoid morphology of the bacteriophage. The possible reason for this morphology could be ‘‘empty’’ or “ghost” virus, where the major axis of the ellipsoid can be 40%

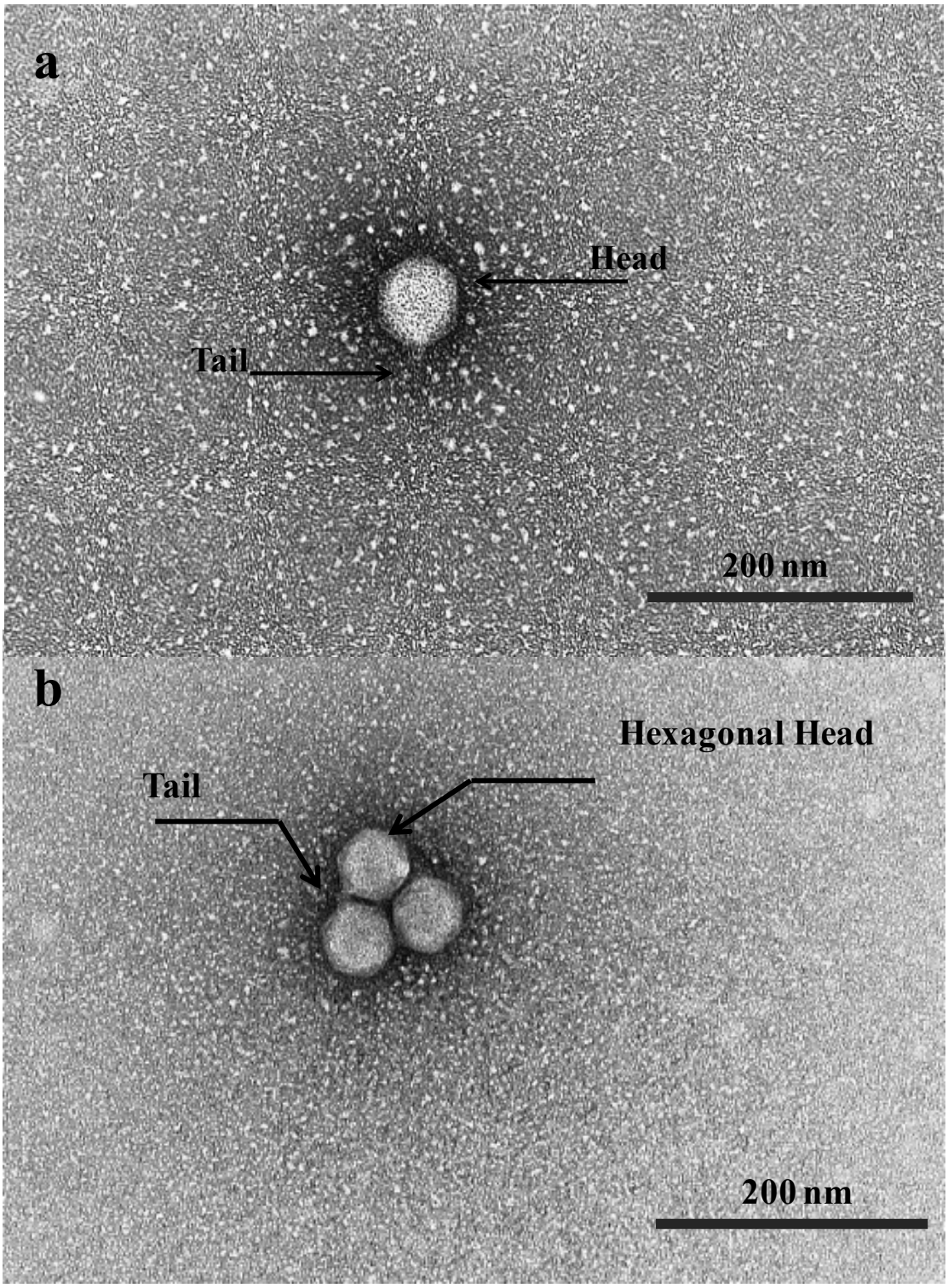

Figure 13. TEM micrographs of the lytic bacteriophage infecting *Chryseobacterium taeanense K-2*

Table 1: The bacteriophage's size obtained from TEM images

Name	image number	Head(nm)	Tail(nm)	Length(nm)
CTP1	123401	77	0	77
CTP1	123402	99	8	107
CTP1	123403	84	6	92
CTP1	123404	93	0	93(89)
CTP2	123393	77	15	92
CTP2	123394	77	15	92
CTP2	123396	77	0	77
CTP3	123397	69	23	92
CTP3	123398	77	0	77
CTP3	123399	84	0	84
CTP3	123400	77	0	77

longer than the minor axis (Pease et al. 2009).

The possible reason for the deformation of the phage could be a result of fixing and staining preparation steps. Similar defects in the viral morphology were reported following the VP2-directed packaging of green fluorescent protein into MPV VLPs (Boura et al. 2005).

3.2.5 One-step growth curve

The replication of bacteriophages during the infection of the host bacterium, *Chryseobacterium taeanense k-2*, was investigated following the method used for *Haliscomenobacter hydrossis* lytic bacteriophages (Kotay et al. 2011). The One-step growth curve of the lytic bacteriophage is depicted in Figure 14. The latent period of *C. taeanense k-2* bacteriophage was found to be around 10 min and the eclipse period and latent period of the virus were synchronized. Latent and eclipse periods are very important parameters for the process of biocontrol. The latent time period spans from the point of phage adsorption to the point at which host lysis occurs and the eclipse time

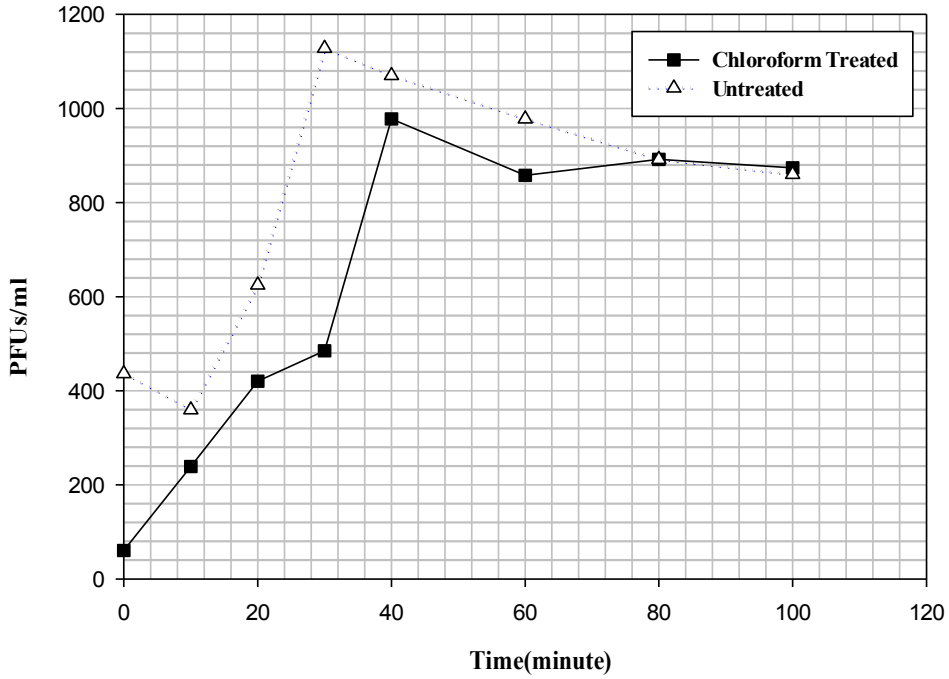

Figure 14. One-step growth curve of lytic bacteriophage infecting *Chryseobacterium taeanense K-2*

period spans from the point of phage adsorption to the point at which the first phage progeny have matured within an infected cell. Following the curve obtained from chloroform treated samples (Figure 14), the trend was not typical as that of previously known phages like T4. It had no initial stable stage which was atypical for any infective virus previously demonstrated (Furness and Fraser 1962). When the bacteriophages infected the cells, they increased immediately until a peak of 1100 PFUs/ml was reached at 40 h. On the other hand, the chloroform untreated curve shows that the initial free bacteriophages was 420 PFUs/ml. In the first 10 min, the bacteriophage numbers were

decreasing due to attachment of the host cells. After 10 min, the bacteriophage numbers were increasing, because of the first lytic cycle completion. The burst size was calculated to be 18±2 PFU/infected cell which was comparable to that of previously reported lytic phages (Kotay et al. 2011).

3.2.6 Phage-to-host ratio analysis

Phage-to-host ratio is critical information necessary for engineering biocontrol applications. Some studies show that a higher phage-to-host ratio (PHR) can cause more than 90% mortality of *H. hydrossis* and VBR lower than 1:1000, resulting in mortality of less than 10% (Kotay et al. 2011). On the other hand, higher PHR does not always represent optimum lytic effect of the bacteriophage on the targeted hosts. For example, over death of filamentous bacteria could cause negative effects on the biomass settleability. Activated sludge bioreactor consists of a complex community of a variety of organisms (Kotay et al. 2011). In general, during the infecting and multiplying processing, bacteriophages have a critical threshold ratio target to the host populations. According to the curve of VLPs versus time (Figure 15) and Live/Dead cells ratio versus time (Figure 16), PHR of 100:1 was found to be most effective, where 98.7% of the host bacterium, *Chryseobacterium taeanense K-2,* were dead. In addition, the final viral count was 7.71E+7 VLPs/ ml after 9 h infection (Table 2.). However, the daughter bacteriophage numbers were found to be decreasing from 4.42E+08 and 1.62E+10 VLPs/ml to 2.65E+8 and 7.09E+8 VLPs/ml, in case of PHRs 1000:1 and 10000:1,

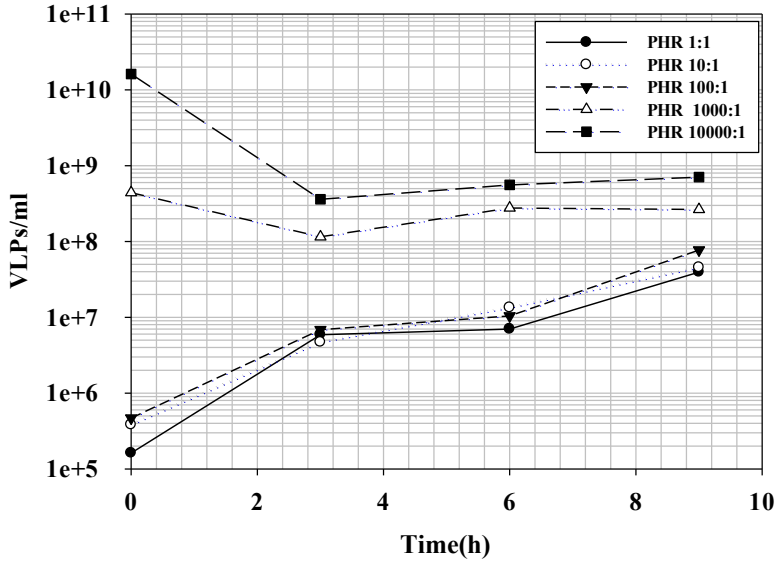

Figure 15. Profile of VLPs at different PHR

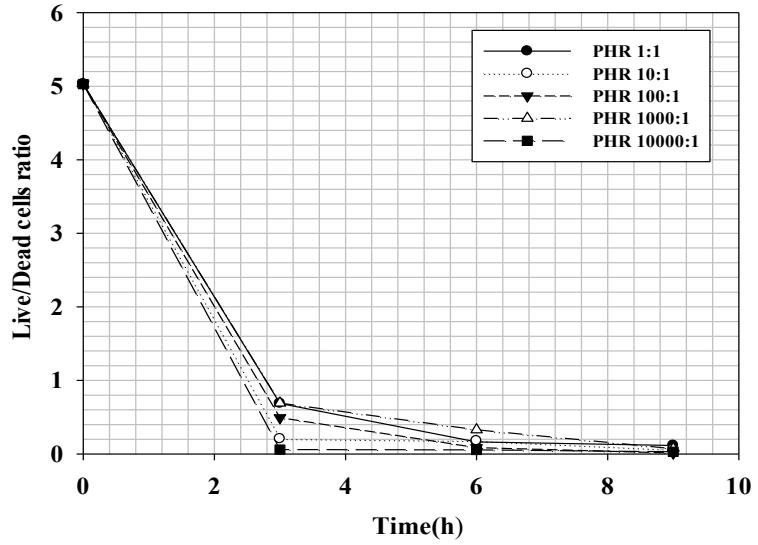

Figure 16. Profile of Live/Dead Cells ratios at different PHR

Table 2: Effect of initial phage/host ratio on bacteriolysis and VLP count

Phage/Host Ratio and Final VLPs after 9 hrs infection			
Initial Phage/ Host ratio	Final O.D.	Final bacteria Live/Dead Ratio	Final VLPs/ml
1:1	0.172	0.1164	3.95E+07
10:1	0.183	0.0581	4.54E+07
100:1	0.193	0.013	7.71E+07
1000:1	0.19	0.709	2.65E+08
10000:1	0.171	0.0299	7.09E+08

respectively. The reduced efficacy at higher phage to host ratio may be because of competitive interference between bacteriophages (Delbrück, 1940); repeated initiation of replication can lyse the bacterium.

This study, however, was limited to plantonic population of *Chryseobacterium taeanense K-2*. Higher PHR might be necessary in case of complex populations of the host like sludge flocs which contain a mixed community of bacteria and biofilms which could have multiple layers of host bacteria. Nevertheless, bacteriophage-based biocontrol is a viable strategy to regulate *Chryseobacterium taeanense K-2* through an application of optimal PHR.

Bacteriophages can also be used in an integrated approach in combination with other biocidal chemicals; however, it is not a panacea to solve all biofilm problems or biofouling in wastewater engineering. Bacteriophage-based biocontrol needs a lot of

preparatory research to determine the most efficacious dosing strategies and the most effective combinations of phages targeting bacterial hosts.

3.3 Biofilms disintegration using phage therapy

3.3.1 Phage therapy for biofilm

Figures 17 a1 and a2 show the 16-day-old biofilm grown on the glass slides stained by Live/Dead BacLight™ and Calcoflour White. The micrographs indicated the morphology of biofilm prior to phage application. The morphologies present in the cells are growing and contacting as "microcolonies" in which the diameter is ranging from 1 to 5 μm. Very faint volumes of extra-polymeric substance (blue fluorescent) were observed. Microcolonies have been known as one of the steps in the development of a biofilm. On the other hand, no "microcolonies" were observed in the biofilm treated with 10^{13} PFUs/ml phages overnight (Figure 17 b1 and b2). This phenomena may attributed to the disruption of the microcolonies following infection by the lytic phage.

Biofilms of the age 54 days were stained in a similar way. Figure 18 indicated that the morphology of biofilm has more cells and complex structure. Micrographs in Figure 18 a1 and a2 show the distributions of live (green) / dead (red) cells and a relatively higher volume/network of EPS than compared to 16-day-old biofilm. Following infection, integrity and uniformity of the biofilm was no longer observed (Figure 18 b1 and b2). Also, the distinct cell structure of the *Chryseobacterium taeanense* K-2 was lost, and cell lysis was evident from the red colored lumps (Figure 18 b1 and b2). This finding further

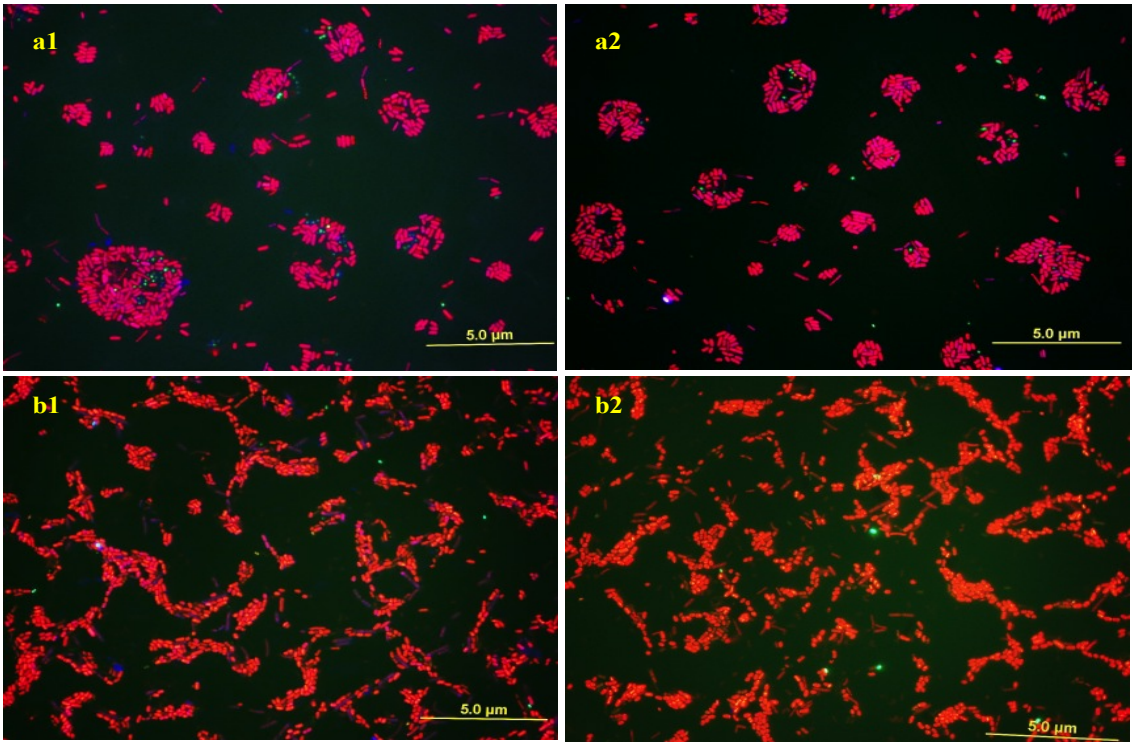

Figure 17. Epifluorescent micrographs of 16-day biofilm (a1 & a2) before and (b1 & b2) after infection with phage.

strengthens the earlier speculation of the feasibility of bacteriophages-based biocontrol of biofilms.

On the contrary, the micrographs obtained from 84-day-old biofilm showed different cellular morphology and higher biovolume of EPS (Figure 19 a1 and a2). Differential cellular morphology of bacteria within a biofilm has been reported earlier. Following application of phage, there were no distinct cells lysis or EPS disintegration observed. It may be speculated that phage was not able to penetrate relatively older biofilm. Biofilms are known to gain complexity, thickness, and impermeability with age

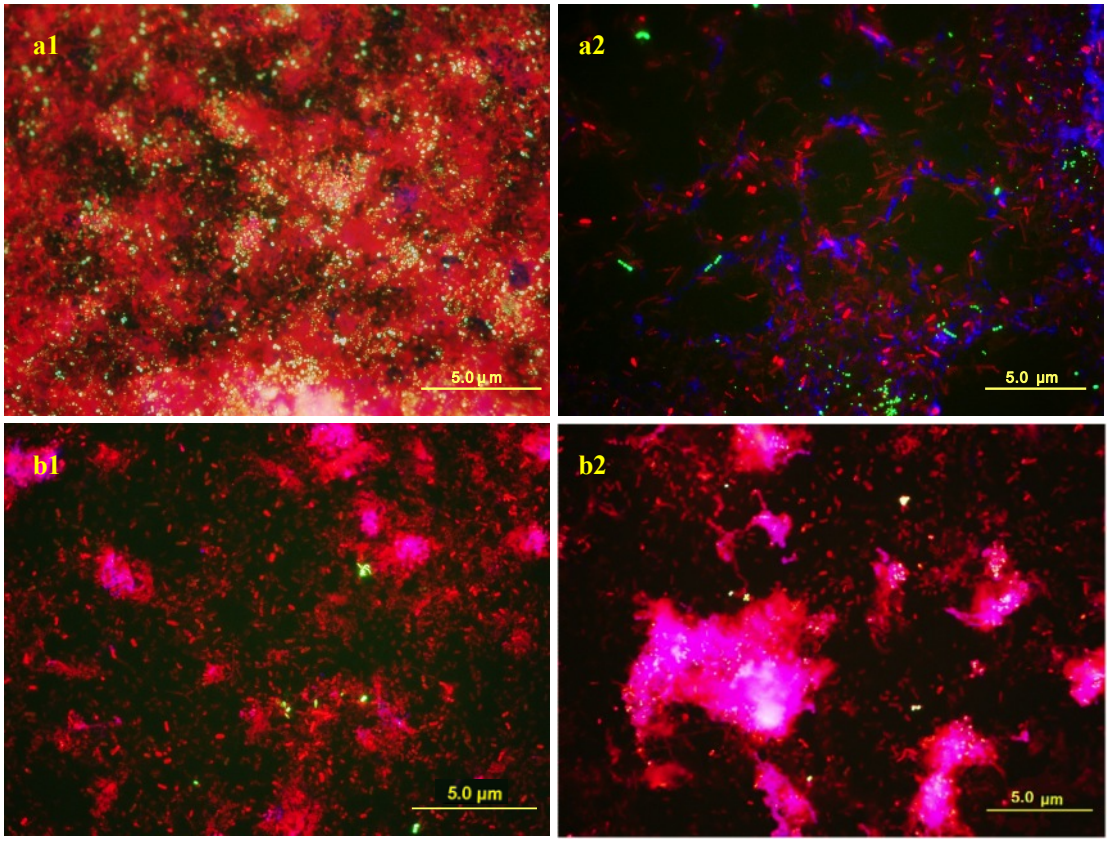

Figure 18. Epifluorescent micrographs of 54-day biofilm (a1 & a2) before and (b1 & b2) after infection with phage.

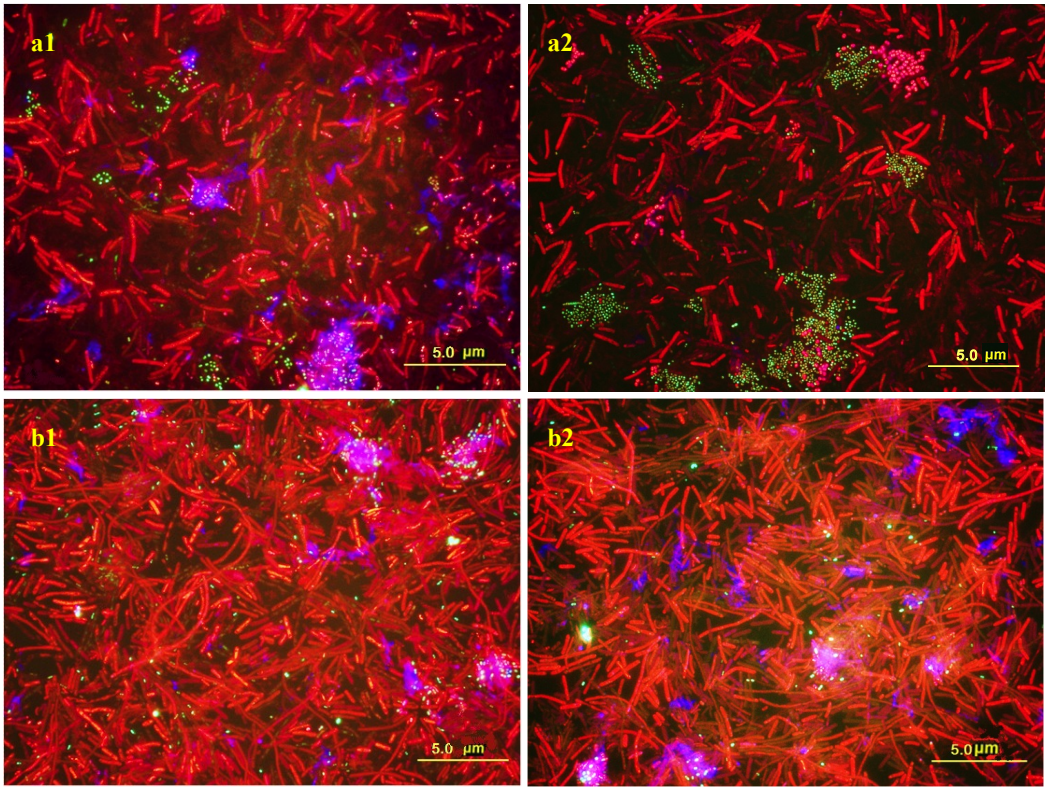

Figure 19. Epifluorescent micrographs of 84-day biofilm (a1& a2) before and (b1 & b2) after infection with phage.

and therefore could resist phage infection. Further investigation will be necessary to understand this phenomenon.

3.3.2 Biofilms quantification using epifluorescence micrographs and BioImageL

BioImageL is an image analysis software widely used for investigation of microbial biofilms. The basic principle is based on in situ color segmentation. BioImageL has the capability to identify and distinguish green (Live) and red (Dead) subareas and calculate different architectural parameters (Figure 20, Figure 21, and Figure 22).

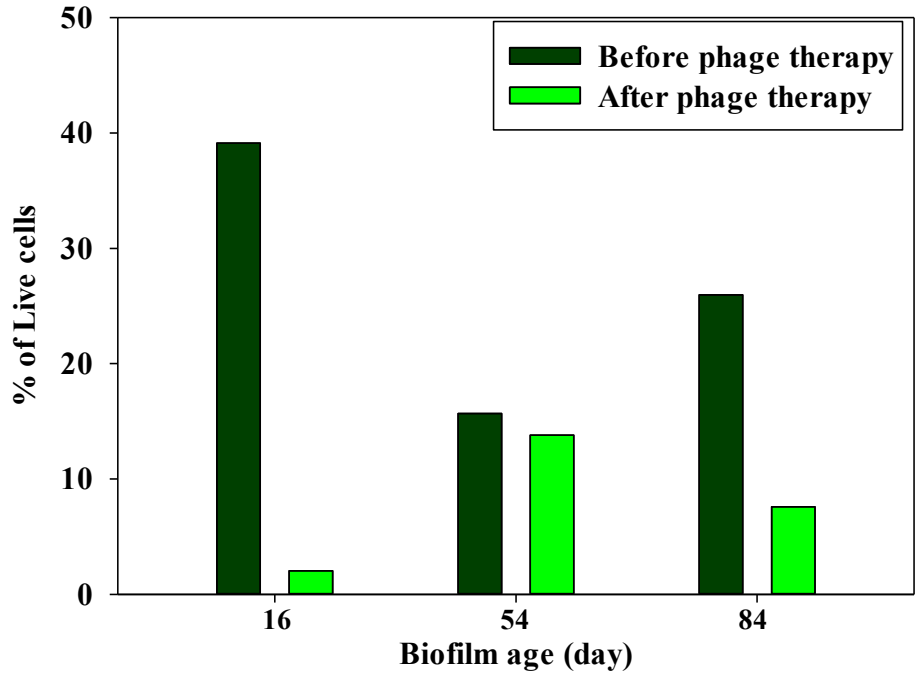

Figure 20. Effect of phage therapy on % Live cells in the biofilm of different ages

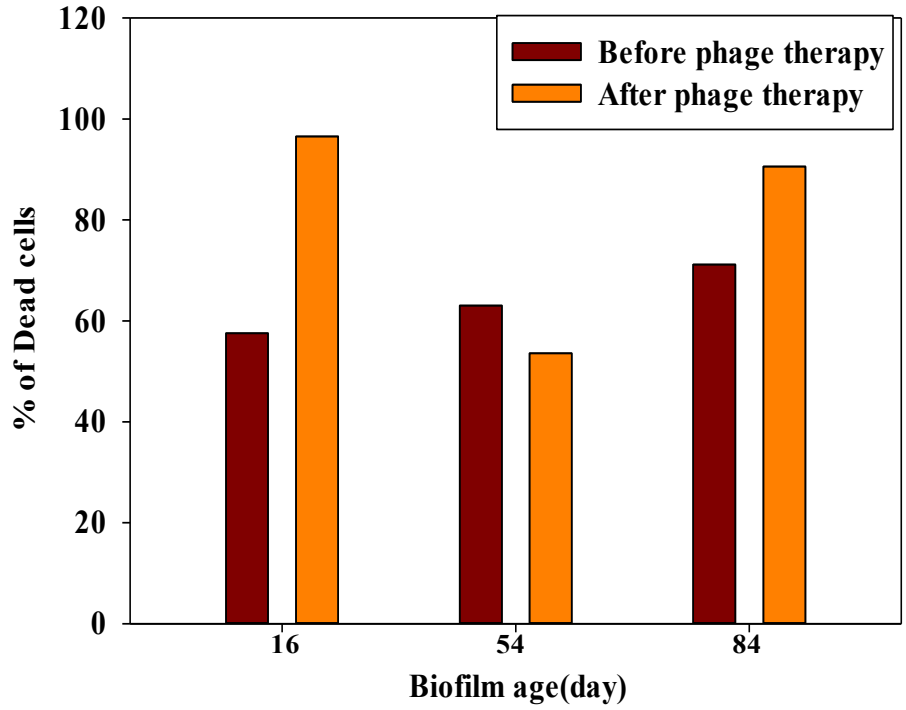

Figure 21. Effect of phage therapy on % Dead cells in the biofilm of different ages

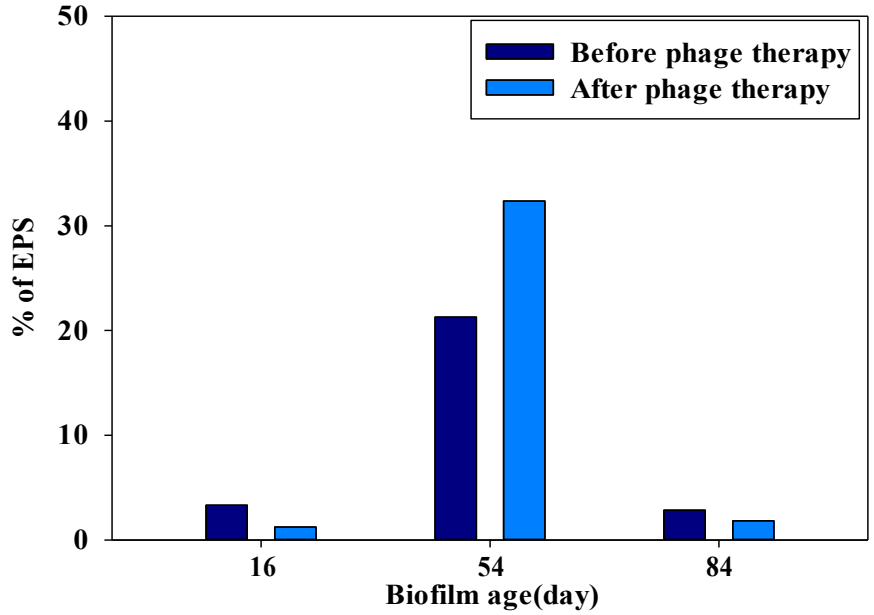

Figure 22. Effect of phage therapy on % EPS in the biofilm of different ages

The percentage of live cells in 16-day-old biofilm decreased from 39.12% to 2.04% following infection with the lytic phage. The percentage of dead cells increased from 57.55% to 96.54% and the percentage of EPS decreased from 3.32% to 1.23% after overnight infection of 16-day biofilm with 10^{13} PFUs/ml.

After overnight phages infection, the percentage of live cells in 54-day-old biofilm decreased from 15.67% to 13.79%, the percentage of dead cells decreased from 63.05% to 53.85%, and the percentage of EPS decreased from 21.28% to 32. 36%.

After overnight phages infection, the percentage of live cells of 84-day biofilm decreased from 25.97% to 7.58%, the percentage of dead cells increased from 71.17% to 90.59%, and the percentage of EPS decreased from 2.84% to 1.82%.

Based on the T-Test analysis on biofilm quantification of 16-day-old biofilm before and after phage infection, the P value of the percentages of Live/Dead cells and EPS

were found to be 0.002, 0.002, and 0.0493, and for 54-day biofilm were found to be 0.463, 0.213, and 0.0095. For 84-day biofilm, they were found to be 1.6857E-08, 1.4486E-08, and 0.063. The possible reason that P value was higher for 16-day and 54-day biofilm (0.463 and 0.213) could be attributed to the fact that there was no adjustment available in the software for the system error even though the noise factors were reduced in the biofilms micrograph during processing. Likewise, further studies are needed for Confocal laser scanning microscopy images analysis to determine the EPS distribution and quantify the thickness of biofilms.

3.3.3 Scanning electron microscope images analysis

Scanning electron microscope (SEM) analysis of biofilm before and after the infection was performed to understand the extent and mechanism of infection at a high resolution. Figure 23 a1 and a2 show the surface structure of the 16-day-old biofilms prior to the phage infection. The structure reveals bacterial cells impregnated within a smooth EPS matrix. Figure 23 b1 and b2 show the surface structure of the 16-day-old biofilms after the phage infection. Hole-like structures were observed throughout the surface of the biofilm. These holes were consistent across the surface of the biofilm which may have emerged due to phage infection. Similar findings were observed in the SEM micrographs of 54-day and 84-day-old biofilms (Figures 24 and 25).

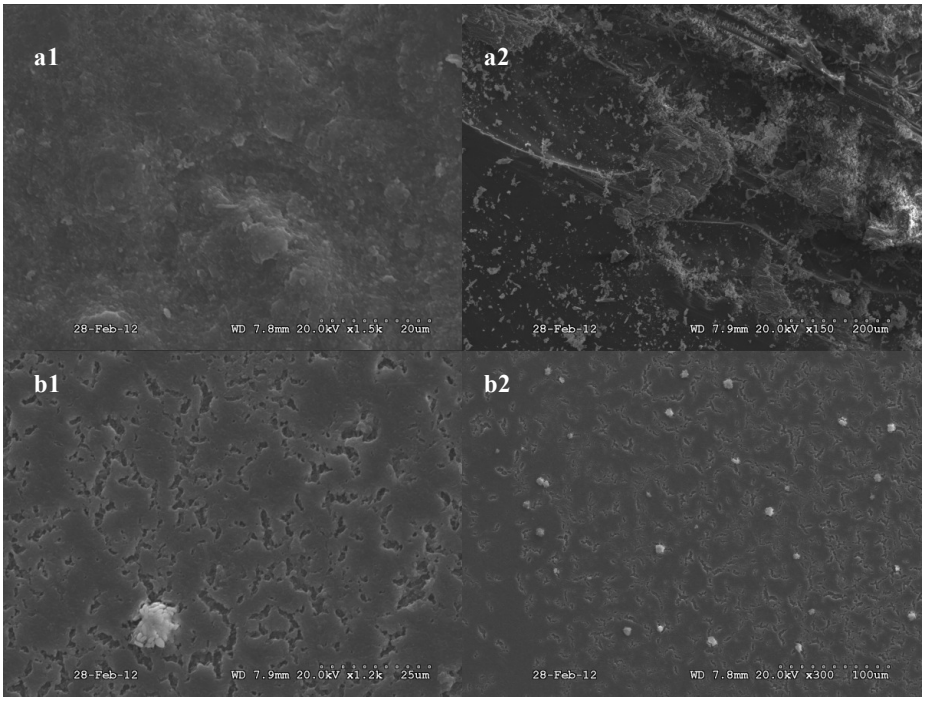

Figure 23. SEM micrographs of 16-day-old biofilm before (a1 & a2) and after (b1 & B2) phage infection

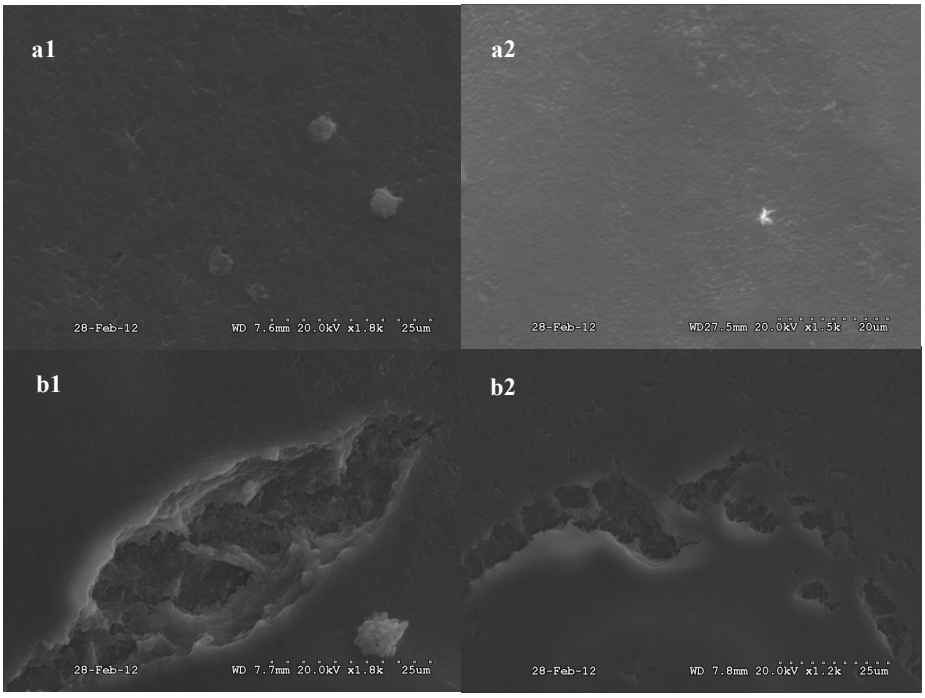

Figure 24. SEM micrographs of 54-day-old biofilm before (a1 & a2) and after (b1 & B2) phage infection

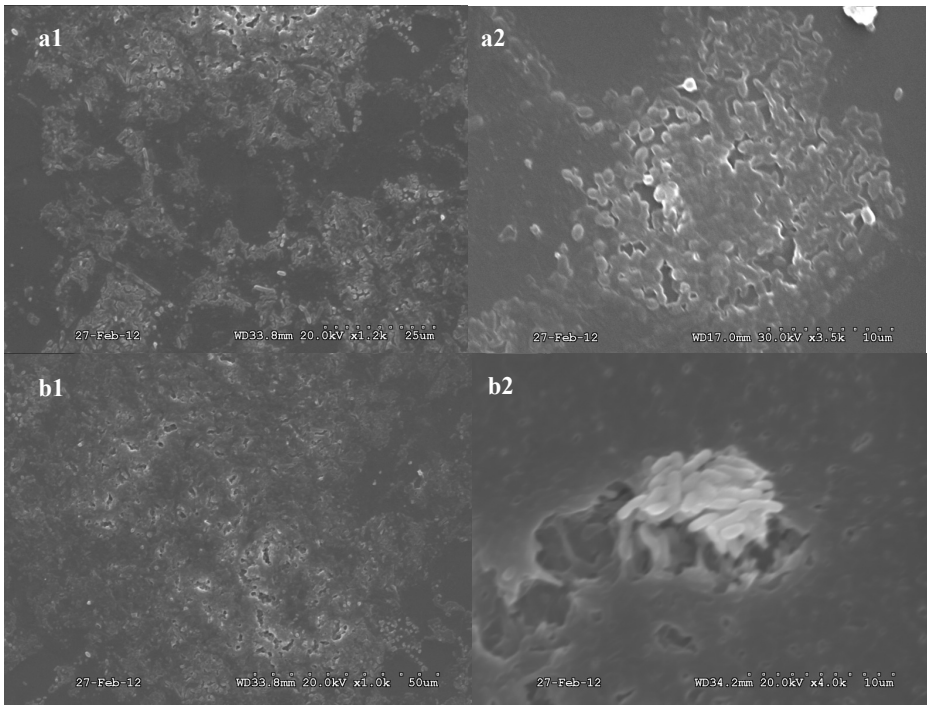

Figure 25. SEM micrographs of 84-day-old biofilm before (a1 & a2) and after (b1 & B2) phage infection

CHAPTER 4

CONCLUSIONS

4.1 Conclusions from study

The goal of this research was to demonstrate bacteriophage-mediated biocontrol of biofilm formed by antibiotic resistant bacterium isolated from a full-scale wastewater treatment plant. Based on the results obtained, the following conclusions can be made:

1. The antibiotic resistant bacterium, *Chryseobacterium taeanense* K-2, was isolated from a wastewater treatment plant. This is the first report on the finding of an antibiotic-resistant strain of *Chryseobacterium taeanense.* The study is also one among the few to have isolated an unconventional antibiotic-resistant bacterium that has not previously been associated with pathogenesis.

2. A lytic bacteriophage specific to *Chryseobacterium taeanense* K-2 existed in the wastewater treatment system and was successfully isolated. The burst size was calculated to be 18±2 PFU/infected cells. Suitable Phage-to-Host ratio for infection was found to be 100:1 which caused the 98.7% death of host planktonic cells.

3. The results of biofilm quantification show that the lytic bacteriophage was able to disintegrate 16 and 54-day-old biofilms of *Chryseobacterium taeanense* K-2, but 84-day-old biofilm did not show a significant difference.

APPENDIX

Table 3: Live/dead cells and EPS distribution of the biofilm of the age of 16 days without phages infected

Biofilm of the Age of 16 days (control)										
Image Number	Noise Reducing Factor	Field Size (um^2)	Cells Area (um^2)	Cells Area covered (%)	Green Cells Area (um^2)	Green Cells (%)	Red Cells Area (um^2)	Red Cells (%)	EPS (um^2)	EPS (%)
1	0.15	45029	5176	11.5	253	4.9	4683	90.5	240	4.6
2	0.09	45029	2926	6.5	214	7.3	2693	92	19	0.6
3	0.1	45029	3634	8.1	156	4.3	3388	93.2	90	2.5
4	0.23	45029	5432	12.1	2988	55	2331	42.9	113	2.1
5	0.26	45029	18844	41.8	15188	80.2	3414	18.1	313	1.7
6	0.29	45029	2767	6.1	1333	48.2	1224	44.2	209	7.6
7	0.2	45029	4617	10.3	590	12.8	3024	65.5	1003	21.7
8	0.04	45029	1897	4.4	308	15.5	1655	83.7	15	0.8
9	0.13	45029	19174	42.6	15801	82.4	2400	12.5	974	5.1
10	0.01	45029	3158	7	1623	51.4	1533	48.5	2	0.1
11	0.31	45029	746	1.7	214	28.7	490	66.9	33	4.4
12	0.39	45029	4333	9.6	3462	79.9	793	18.3	78	1.8
13	0.16	45029	822	1.8	566	68.8	251	30.5	5	0.6
14	0.09	45029	194	0.4	93	47.9	100	51.5	1	0.6
15	0.09	45029	162	0.4	56	34.7	105	64.8	1	0.4
16	0.05	45029	419	0.9	91	21.7	328	78.1	1	0.2
17	0.05	45029	826	1.8	41	5	782	94.7	3	0.3
18	0.05	45029	398	0.9	124	31.1	273	68.5	2	0.4
19	0.03	45029	1980	4.4	1131	57.1	843	42.6	6	0.3
20	0.29	45029	163	0.4	68	41.8	82	50.5	12	7.6
21	0.15	45029	992	2.2	28	2.8	963	97.1	1	0.1
22	0.05	45029	1353	3	509	37.7	831	61.4	12	0.9
23	0.09	45029	644	1.4	37	5.8	606	94.2	0	0.1
24	0.06	45029	938	2.1	558	60.1	341	36.8	29	3.1
25	0.03	45029	525	1.2	420	80	86	16.3	19	3.7
26	0.03	45029	2000	4.4	152	7.6	1844	92.2	4	0.2
27	0.03	45029	656	1.5	344	52.4	301	45.9	11	1.7
28	0.06	45029	989	2.2	590	59.7	386	39	13	1.3
29	0.01	45029	462	1	299	64.6	147	31.7	17	3.6
30	0.32	45029	2371	5.3	1490	62.8	296	12.5	585	24.7
31	0.07	45029	1251	2.8	6	0.5	1244	99.5	0	0
Average			2898.355	6.445161	1572.032	39.11935	1207.645	57.55161	122.9355	3.316129

Table 4: Live/dead cells and EPS distribution of the biofilm of the age of 16 days with phages infected

Biofilm of the Age of 16 days (infected)										
Image Number	Noise Reducing Factor	Field Size (um^2)	Cells Area (um^2)	Cells Area covered (%)	Green Cells Area (um^2)	Green Cells (%)	Red Cells Area (um^2)	Red Cells (%)	EPS (um^2)	EPS (%)
1	0.07	45029	7407	16.4	27	0.4	6982	94.3	398	0.4
2	0.07	45029	8381	18.6	8	0.1	8287	98.9	86	1
3	0.11	45029	869	1.9	33	3.8	821	94.6	14	1.6
4	0.11	45029	171	0.4	7	4.1	156	91.6	7	4.3
5	0.01	45029	435	1	15	3.5	420	96.4	0	0
6	0.27	45029	3357	7.5	203	6.1	3054	91	100	3
7	0.21	45029	10249	22.8	2187	21.3	7547	73.6	515	5
8	0.24	45029	1483	3.3	55	3.7	1353	91.3	75	5
9	0.35	45029	2831	6.3	53	1.9	2683	94.8	95	3.3
10	0.34	45029	6694	14.9	476	7.1	6065	90.6	152	2.3
11	0.1	45029	5245	11.6	90	1.7	5147	98.1	9	0.2
12	0.07	45029	5576	12.4	26	0.5	5538	99.3	12	0.2
13	0.06	45029	3894	8.6	30	0.8	3863	99.2	1	0
14	0.07	45029	3227	7.2	21	0.6	3200	99.1	7	0.2
15	0.07	45029	5385	12	62	1.2	5307	98	15	0.3
16	0.05	45029	5424	12	4	0.1	5415	99.8	5	0.1
17	0.05	45029	5765	12.8	22	0.4	5724	99.3	19	0.3
18	0.05	45029	1612	3.6	5	0.3	1606	99.7	0	0
19	0.05	45029	4421	9.8	12	0.3	4409	99.7	0	0
20	0.05	45029	3212	7.1	10	0.3	3197	99.5	5	0.2
21	0.09	45029	1416	3.1	22	1.6	1392	98.3	1	0.1
22	0.05	45029	11346	25.2	21	0.2	10425	91.9	900	7.9
23	0.05	45029	3813	8.5	8	0.2	3804	99.8	1	0
24	0.05	45029	6074	13.5	24	0.4	6044	99.5	6	0.1
25	0.05	45029	6256	13.9	6	0.1	6247	99.8	4	0.1
26	0.05	45029	7520	16.7	33	0.4	7481	99.5	6	0.1
27	0.05	45029	3470	7.7	37	1.1	3425	98.7	8	0.2
28	0.05	45029	2884	6.4	0	0	2879	99.8	5	0.2
29	0.05	45029	6133	13.6	9	0.1	6122	99.8	2	0
30	0.05	45029	1714	3.8	5	0.3	1708	99.6	1	0
31	0.05	45029	3381	7.5	21	0.6	3292	97.4	67	2
Average			4504.677	10.00323	113.9355	2.03871	4309.452	96.54516	81.16129	1.229032

Table 5: Live/dead cells and EPS distribution of the biofilm of the age of 54 days without phages infected

Biofilm of theAge of 54 days (control)										
Image Number	Noise Reducing Factor	Field Size (um^2)	Cells Area (um^2)	Cells Area covered (%)	Green Cells Area (um^2)	Green Cells (%)	Red Cells Area (um^2)	Red Cells (%)	EPS (um^2)	EPS (%)
1	0.09	45029	2358	5.2	1348	57.1	630	26.7	380	16.1
2	0.55	45029	2793	6.2	380	13.6	1921	68.8	491	17.6
3	0.2	45029	4950	11	1982	40	1620	32.7	1348	27.2
4	0.16	45029	4213	9.4	312	7.4	3295	78.2	605	14.4
5	0.14	45029	10614	23.6	1984	18.7	4053	38.2	4578	43.1
6	0.23	45029	5181	11.5	243	4.7	4557	88	381	7.3
7	0..1	45029	785	1.7	106	13.5	435	55.5	244	31
8	0.22	45029	8983	19.9	884	9.8	5999	66.8	2100	23.4
9	0.2	45029	45029	100	8990	19.7	29318	64.1	7407	16.2
10	0.17	45029	8107	18	5045	62.2	2265	27.9	797	9.8
11	0.13	45029	14230	31.6	904	6.4	10971	77.1	2355	16.6
12	0.21	45029	31322	69.6	12489	39.9	12331	39.4	6502	20.8
13	0.11	45029	45044	100	0	0	44392	98.6	647	1.4
14	0.13	45029	7918	17.6	408	5.2	7435	93.9	75	0.9
15	0.17	45029	2833	6.3	382	13.5	1129	39.9	1322	46.7
16	0.16	45029	4387	9.7	343	7.8	3007	68.6	1036	23.6
17	0.19	45029	10525	23.4	164	1.6	9424	89.5	937	8.9
18	0.23	45029	12010	26.7	4483	37.3	5849	48.7	1678	14
19	0.24	45029	14137	31.4	6274	44.4	5311	37.6	2551	18
20	0.39	45029	4818	10.7	1051	21.8	3042	63.1	725	15
21	0.34	45029	2611	5.8	533	20.4	583	22.3	1494	57.2
22	0.47	45029	1466	3.3	279	19	795	54.3	392	26.7
23	0.29	45029	11534	25.6	6	0.1	11082	96.2	435	3.8
24	0.12	45029	7549	16.8	1211	16	3330	44.1	3008	39.9
25	0.11	45029	31062	69	3330	10.7	15303	49.3	12429	40
26	0.19	45029	8959	19.9	54	0.6	8709	97.2	196	2.2
27	0.29	45029	14916	33.1	6	0	13483	90.4	1428	9.6
28	0.18	45029	5572	12.4	438	7.9	3384	60.7	1750	31.4
29	0.27	45029	15994	35.5	4111	25.7	3871	24.2	8013	50.1
30	0.29	45029	45413	100	0	0	35905	79.1	9507	20.9
31	0.25	45029	26779	59.5	553	2.1	26007	97.1	220	0.8
Average			13657.8	30.30667	1898.167	15.66667	9293.533	63.05	2488.367	21.28333

Table 6: Live/dead cells and EPS distribution of the biofilm of the age of 54 days with phages infected

Biofilm of theAge of 54 days (infected)										
Image Number	Noise Reducing Factor	Field Size (um^2)	Cells Area (um^2)	Cells Area covered (%)	Green Cells Area (um^2)	Green Cells (%)	Red Cells Area (um^2)	Red Cells (%)	EPS (um^2)	EPS (%)
1	0.2	45029	12898	28.6	332	2.6	9763	75.7	2803	21.7
2	0.05	45029	22441	49.8	3913	17.4	11384	50.7	7145	31.8
3	0.2	45029	2248	5	176	7.9	1639	72.9	432	19.2
4	0.07	45029	13970	31	5426	38.8	3894	27.9	4649	33.3
5	0.11	45029	8158	18.1	5988	73.4	502	6.2	1668	20.4
6	0.16	45029	3414	7.6	75	2.2	2820	82.6	519	15.2
7	0.23	45029	5313	11.8	69	1.3	4290	80.7	954	18
8	0.15	45029	6187	13.7	621	10	1383	22.4	4182	67.6
9	0.29	45029	4433	9.8	28	0.6	1889	42.6	2516	56.8
10	0.47	45029	6928	15.4	2743	39.6	2574	37.2	1611	23.2
11	0.19	45029	8340	18.5	75	0.9	7354	88.2	910	10.9
12	0.28	45029	29845	66.3	2	0	28046	94	1797	6
13	0.11	45029	1971	4.4	80	4.1	1421	72.1	469	23.8
14	0.19	45029	8248	18.3	651	7.9	6640	80.5	957	11.6
15	0.07	45029	8371	18.6	2276	27.2	1892	22.6	4204	50.2
16	0.11	45029	14042	31.2	3665	26.1	5545	39.5	4832	34.4
17	0.18	45029	7110	15.8	117	1.6	5842	82.2	1151	16.2
18	0.18	45029	10085	22.4	570	5.7	6801	67.4	2714	26.9
19	0.2	45029	6694	14.9	629	9.4	3909	58.4	2156	32.2
20	0.2	45029	3799	8.4	7	0.2	1756	46.2	2037	53.6
21	0.25	45029	4632	10.3	1911	41.3	513	11.1	2208	47.7
22	0.11	45029	670	1.5	168	25.1	136	20.4	365	54.5
23	0.19	45029	15305	34	64	0.4	12030	78.6	3211	21
24	0.18	45029	5255	11.7	110	2.1	2562	48.8	2583	49.1
25	0.09	45029	8817	19.6	1282	14.5	3935	44.6	3600	40.8
26	0.14	45029	13323	29.6	117	0.9	10964	82.3	2242	16.8
27	0.14	45029	14787	32.8	2779	18.8	7472	50.5	4536	30.7
28	0.16	45029	5668	12.6	294	5.2	2820	49.8	2554	45.1
29	0.11	45029	5042	11.2	266	5.3	1227	24.3	3549	70.4
30	0.15	45029	9083	20.2	2115	23.3	5001	55.1	1967	21.7
31		45029								
Average			8902.567	19.77	1218.3	13.79333	5200.133	53.85	2484.033	32.36

Table 7: Live/dead cells and EPS distribution of the biofilm of the age of the 84 days without phages infected

Biofilm of the Age of 84 days (control)										
Image Number	Noise Reducing Factor	Field Size (um^2)	Cells Area (um^2)	Cells Area covered (%)	Green Cells Area (um^2)	Green Cells (%)	Red Cells Area (um^2)	Red Cells (%)	EPS (um^2)	EPS (%)
1	0.36	45029	26331	58.5	405	1.5	25239	95.9	687	2.6
2	0.11	45029	12944	28.7	1857	14.3	10982	84.8	105	0.8
3	0.25	45029	27933	62	13039	46.7	14298	51.2	596	2.1
4	0.13	45029	26207	58.2	2870	11	23193	88.5	144	0.5
5	0.34	45029	23386	51.9	6059	25.9	16709	71.4	618	2.6
6	0.23	45029	33829	75.1	615	1.8	32719	96.7	496	1.5
7	0.41	45029	23716	52.7	12271	51.7	8946	37.7	2498	10.5
8	0.08	45029	40311	89.5	28619	71	11171	27.7	522	1.3
9	0.42	45029	37527	83.3	19321	51.5	16281	43.4	1925	5.1
10	0.11	45029	8478	18.8	355	4.2	7871	92.8	252	3
11	0.15	45029	27932	62	851	3	25679	91.9	1402	5
12	0.03	45029	21223	47.1	271	1.3	20744	97.7	208	1
13	0.12	45029	31103	69.1	900	2.9	29793	95.8	410	1.3
14	0.14	45029	5467	12.1	50	0.9	5417	99.1	0	0
15	0.44	45029	34903	77.5	19500	55.9	14494	41.5	909	2.6
16	0.12	45029	45029	100	327	0.7	42766	94.5	2164	4.8
17	0.28	45029	42687	94.8	4553	10.7	35184	82.4	2950	6.9
18	0.03	45029	39305	87.3	20223	51.5	18789	47.8	293	0.7
19	0.18	45029	41011	91.1	18047	44	22215	54.2	748	1.8
20	0.23	45029	41280	91.7	18823	45.6	21521	52.1	936	2.3
21	0.02	45029	35687	79.3	13281	37.2	21893	61.3	514	1.4
22	0.13	45029	35246	78.3	5751	16.3	29086	82.5	408	1.2
23	0.06	45029	30751	68.3	7546	24.5	22298	72.5	907	2.9
24	0.13	45029	10872	24.1	2964	27.3	7820	71.9	88	0.8
25	0.17	45029	43561	96.7	12454	28.6	29809	68.4	1298	3
26	0.01	45029	35730	79.3	19251	53.9	13599	38.1	2880	8.1
27	0.09	45029	42202	93.7	2792	6.6	39138	92.7	272	0.6
28	0.1	45029	11460	25.5	1928	16.8	9171	80	362	3.2
29	0.14	45029	29044	64.5	11901	41	15904	54.8	1238	4.3
30	0.23	45029	23357	51.9	15306	65.5	6988	29.9	1063	4.6
31	0.24	45029	25446	56.5	636	2.5	24369	95.8	440	1.7
32	0.42	45029	13827	30.7	4753	34.4	8359	60.5	715	5.2
33	0.25	45029	26785	59.5	1654	6.2	24970	93.2	161	0.6
Average			28926.36	64.23333	8156.758	25.96667	19921.67	71.17273	854.8182	2.848485

Table 8: Live/dead cells and EPS distribution of the biofilm of the age of the 84 days with phages infected

Biofilm of the Age of 84 days (infected)										
Image Number	Noise Reducing Factor	Field Size (um^2)	Cells Area (um^2)	Cells Area covered (%)	Green Cells Area (um^2)	Green Cells (%)	Red Cells Area (um^2)	Red Cells (%)	EPS (um^2)	EPS (%)
1	0.17	45029	44860	99.6	4	0	43963	98	893	2
2	0.05	45029	22272	49.5	2898	13	18086	81.2	1288	5.8
3	0.35	45029	29591	66.7	2515	8.5	26274	88.8	802	2.7
4	0.32	45029	14722	32.7	189	1.3	14154	96.1	380	2.6
5	0.18	45029	7500	16.7	351	4.7	7135	95.1	15	0.2
6	0.23	45029	9894	22	74	0.8	9105	92	715	7.2
7	0.32	45029	31050	69	49	0.2	29869	96.2	1133	3.6
8	0.1	45029	45088	100	142	0.3	43275	96	1671	3.7
9	0.1	45029	29385	65.3	94	0.3	29256	99.6	35	0.1
10	0.17	45029	42430	94.2	2871	6.8	38678	91.2	881	2.1
11	0.12	45029	42241	93.8	2750	6.5	39316	93.1	175	0.4
12	0.17	45029	22817	50.7	99	0.4	22616	99.1	103	0.5
13	0.14	45029	23575	52.4	186	0.8	22510	95.5	879	3.7
14	0.21	45029	18967	42.1	154	0.8	18721	98.7	92	0.5
15	0.07	45029	14021	31.1	295	2.1	13547	96.6	179	1.3
16	0.08	45029	12712	28.2	643	5.1	12051	94.8	18	0.1
17	0.22	45029	32247	71.6	11	0	31099	96.4	1138	3.5
18	0.14	45029	35014	77.8	1838	5.3	32768	93.6	407	1.2
19	0.13	45029	20479	45.5	1060	5.2	19401	94.7	18	0.1
20	0.11	45029	39109	86.9	148	0.4	38756	99.1	204	0.5
21	0.09	45029	34818	77.3	937	2.7	33433	96	449	1.3
22	0.17	45029	38211	84.9	3331	8.7	33950	88.8	939	2.5
23	0.12	45029	45365	100	25031	55.2	19893	43.9	440	1
24	0.15	45029	35636	79.1	776	2.2	34187	95.9	673	1.9
25	0.13	45029	29577	65.7	369	1.2	29146	98.5	62	0.2
26	0.18	45029	44678	99.2	3972	8.9	39580	88.6	1125	2.5
27	0.12	45029	35442	78.7	987	2.8	34319	96.8	136	0.4
28	0.11	45029	35146	78.1	24746	70.4	9727	27.7	673	1.9
29	0.09	45029	9146	20.3	259	2.8	8743	95.5	153	1.7
30	0.17		17193	38.2	4897	28.5	11756	68.4	540	3.1
31	0.16		33503	74.4	71	0.2	33263	99.3	169	0.5
32	0.05		16613	36.9	367	2.2	16091	96.9	155	0.9
33	0.15		37587	83.5	735	2	36642	97.5	209	0.6
Average			28814.82	64.00303	2510.576	7.584848	25797.27	90.59394	507.5455	1.827273

REFERENCES

Amini, S., and Tavazoie, S. (2011). "Antibiotics and the post-genome revolution." *Curr Opin Microbiol*, 14, 513-518.

Ash, J. R., Mauck, B., and Melissa, M. M. (2002). "Antibiotic resistance of gram-negative bacteria in rivers." *United States*, 8, 713-716.

Bisht, R., Katiyar, A., Singh, R., and Mittal, P. (2009). "Antibiotic resistance- a global issue of concern." *Asian Journal of Pharmaceutical and Clinical Research*, 2, 34-39.

Boura, E., Liebl, D., Spisek, R., Fric, J., Marek, M., Stokrova, J., Holan, V., and Forstova, J. (2005). "Polyomavirus EGFP-pseudocapsids: Analysis of model particles for introduction of proteins and peptides into mammalian cells." *FEBS Letters*, 579,6549–6558.

Breithaupt, H.(1999). "The new antibiotics." *Nat Biotechnol*. 17, 1165–1169.

Bremer, P. J., Fillery, S., and McQuillan, A. J. (2006). "Laboratory scale clean-in-place (CIP) studies on the effectiveness of different caustic and acid wash steps on the removal of dairy biofilms." *Food Microbiology*,106, 254–262.

Breyers, J. D., and Ratner, J. P. (2004). "Bioinspired implant materials befuddle bacteria." *ASM News*, 70, 232–237.

Bumpus, J. and Brock, B., (2004). "Biodegradation of crystal violet by the white rot fungus phanerochaete chrysoporium." *Environmental Protection Agency*, 600, 163.

Carpentier, B., and Cerf, O. (1993). "Biofilms and their consequences with particular references to hygiene in the food industry." *Applied Bacteriology*, 75, 499- 511.

Chang, C. C., Tseng, S. K., Chang, C. C., and Ho, C. M. (2004). "Degradation of 2-chlorophenol via a hydrogenotrophic biofilm under different reductive conditions."

Chemosphere, 56, 989-997.

Chmielewsky，R.A.N., and FranK, J.F. (2003). "Biofilm formation and control in food processing facilities." *Comprehensive Reviews in Food Science and Food Safety*, 2, 22-32.

Darveau, R. P., Tanner, A., and Page, R. C. (2000). "The microbial challenge in periodontitis." *Periodont*, 14**,** 12–32.

Davies, J. (1994). " Inactivation of antibiotics and the dissemination of resistance genes." *Science*, 264, 375–382.

Delbrück, M. (1940). "Adsorption of bacteriophage under variousphysiological conditions of the host." *Journal of General Physiology*, 23, 643-660.

Ellis, E.L., and Delbrück, M. (1939). "The growth of bacteriophage." *Journal of General Physiology*, 22, 365-384.

Eriksson, M., Dalhammar, G., and Mohn, W. W. (2002). "Bacterial growth and biofilm production on pyrene." *FEMS Microbiology Ecology*, 40, 21-27.

Fischbach, M.A., and Walsh C.T. (2009). "Antibiotics for emerging pathogens." *Science*, 325, 1089–1093.

Flint, S. H., Bremer, P. J., and Brooks, J. D. (1997). "Biofilms in dairy manufacturing plant description, current concerns and methods of control." *Biofouling*, 11, 81–97.

Furness, G.B., and Fraser, F. E. (1962). "One-step Growth Curves for Inclusion Blennorrhoea Virus in HeLa Cell Monolayers." *Journal of General Microbiology*, 27, 200-304.

Gilbert, P., Allison, D., and McBain, A. (2002). "Biofilms in vitro and in vivo: Do singular mechanisms imply cross-resistance?" *Journal of Applied Microbiology*, 92, 98-110.

Gill, J.J., Hyman P. (2009). "Phage choice, isolation, and preparation for phage therapy." *Curr Pharm Biotechno*l, 11, 2–14.

Golovlev E.L. (2002). "The mechanism of formation of pseudomonas aeruginosa biofilm, a type of structured population." *Microbiology*, 71 (3), 249 254.

González Ribas F. (2005). Desarrollo y aplicación de sensores para evaluar la contaminación microbiológica de superficies domésticas españolas y de la efectividad de desinfectantes in situ de productos limpiadores comerciales.

Gristina, A.G., Shibata, Y., Giridhar, G., Kreger, A., and Myrvik, Q. N. (1994). "The glycocalyx, biofilm, microbes, and resistant infection." *Seminars in Arthroplasty*, 5, 160–70.

Guibaud, G., van Hullebusch, E., and Bordas, F. (2006). "Lead and cadmium biosorption by extracellular polymeric substances (EPS) extracted from activated sludges: pH-sorption edge tests and mathematical equilibrium modelling." *Chemosphere*, 64, 1955-1962.

Haggag, M. W. (2010). "The role of biofilm exopolysaccharides on biocontrol of plant diseases." *Biopolymers* , 271-275.

Huang, C. H., Renew, J. E., Smeby, K. L., Pinkerston, K., and Sedlak, D.L. (2001). "Assessment of potential antibiotic contaminants in water and preliminary occurrence analysis." *Journal of Contemporary Water Resource Update*, 120, 30–40.

Hyde, J. A., Darouiche, R. O., and Costerton, J. W. (1998). "Strategies for prophylaxis against prosthetic valve endocarditis: A review article." *Journal of Heart Valve Disease* , 7, 313–15.

Jin, G., and Englande, A. J. (1998). "Carbon tetrachloride biodegradation in a fixed-biofilm reactor and its kinetic study." *Water Science and Technology*, 38, 155-162.

Joshua, G. W., Guthrie-Irons, C., Karlyshev, A. V. and Wren, B. W. (2006). "Biofilm formation in Campylobacter jejuni." *Microbiology* , 152, 387- 396.

Judd, S. (2006). *The MBR book principles and applications of membrane bioreactors in water and wastewater treatment*, Elsevier, Oxford.

Kargi, F. and Eker, S. (2005). "Removal of 2, 4-dichlorophenol and toxicity from synthetic wastewater in a rotating perforated tube biofilm reactor." *Process Biochemistry*, 40, 2105-2111.

Kay, E., Vogel, T. M., Bertolla, F., Nalin, R. and Simonet, P. (2002). "In situ transfer of antibiotic resistance genes from transgenic (transplastomic) tobacco plants to bacteria." *Environment Microbiology*, 68, 3345-3351.

Keskinen, L. A., Todd, E.C., and Ryser, E.T. (2008). "Transfer of surface dried *Listeria monocytogenes* from stainless steel knife blades to roast turkey breast." *Food Protection*, 71,176-181.

Kutateladze, M., & Adamia, R. (2010). "Bacteriophages as potential new therapeutics to replace or supplement antibiotics." *Trends in Biotechnology*, 28, 591-595.

Lawrence, J. R., Korber, D. R., Hoyle, B. D., (1991). "Costerton, J. W., and Caldwell, D. E. Optical sectioning of microbial biofilms." *Bacteriology*, 173, 6558-6567.

Lazarova, V., and Manem, J. (2000). "Innovative biofilm treatment technologies for water and wastewater treatment." *Selected Abstracts in Chemistry*, 31, 159-206.

Levy, S. B. (2002). "Factors impacting on the problem of antibiotic resistance."*Antimicrob Chemother*, 49, 25-30.

Marques, S. C., Rezende, J. G. O. S., Alves, L. A. F., Silva, B. C., Alves, E., Abreu, L. R., et al. (2007). "Formation of biofilms by Staphylococcus aureus on stainless steel and glass surfaces and its resistance to some selected chemical sanitizers." *Brazilian Journal of Microbiology*, 38,538–543.

Mattila Sandholm T., and Wirtanen G. (1999). "Biofilm formation in the industry: A review." *Food Reviews International*, 8, 573 603.

Madigan, T. M., John M. Martinko., David A. Stahl, D. A., and Clark, D. P. (2010). *Biology of Microorganisms*, *Pearson Education*, 118.

Madigan, T. M., John M. Martinko., David A. Stahl, D. A., and Clark, D. P. (2010). *Biology of Microorganisms*, *Pearson Education*, 125.

Mittelman, M. W. (1998). "Structure and functional characteristics of bacterial biofilms in fluid processing operations." *Dairy Science* , 81, 2760–2764.

Morris, N. S., Stickler, D. J., and McLean, R. J. (1999). "The development of bacterial biofilms on indwelling urethral catheters." *World Journal Urology*, 17, 345–50.

Naik, G. A., Bhat, L. N., Chpoade, B. A. and Lynch, J. M. (1994). "Transfer of broad-host-range antibiotic resistance plasmids in soil microcosms." *Current. Microbiology* , 28, 209-215.

Ngwai, Y. B., Adachi, Y., Ogawa, Y. and Hara, H. (2006). "Characterization of biofilm-forming abilities of antibiotic resistant *Salmonella typhimurium* DT104 on hydrophobic abiotic surfaces." *Journal of Microbiology, Immunology, and Infection*, 39: 278–291.

O'Toole, G., Kaplan, H. B. and Kolter, R. (2000). "Biofilm formation as microbial Development, Annu. Rev." *Microbiol* , 54, 49–79.

Pace, L. John., Rupp, E. Mark., and Finch, G. Roger. (2006). "Common biofilm-forming microbial pathogens." *Biofilms, Infection, and Antimicrobial Therapy*, 21, 401-402.

Parisien, A., Allain, B., Zhang, J., Mandeville, R., and Lan, C. Q. (2008). "Novel alternatives to antibiotics: Bacteriophages, bacterial cell wall hydrolases, and antimicrobial peptides." *Journal of Applied Microbiology*, 104, 1–13.

Passerini, L., Lam, K., Costerton, J. W., and King, E. G. (1992). "Biofilms on indwelling vascular catheters." *Critical Care Medicine*, 20, 665–73.

Pearl, S., Gabay, C., Kishony, R., Oppenheim, A. and Balaban, N.Q. (2008). "Nongenetic individuality in the host –phage interaction." *PLoS Biology*, 6, 120.

Pease, F. L., Lipin, D. I., Tsai, D. H., Zachariah, R. M., Lua, H. L. L., Tarlov, J. M., and Middelberg, P. J. A. (2009). "Quantitative characterization of virus-like particles by asymmetrical flow field flow fractionation, electrospray differential mobility analysis, and transmission electron microscopy." *Biotechnology & Bioengineering*, 102, 845-855.

Rodgers, M., and Zhan, X. M. (2003). "Moving-medium biofilm reactors." *Reviews in Environmental Science and Biotechnolog*y, 2, 213-224.

Rosén, M., Welander, T., Löfqvist, A., and Holmgren, J. (1998). "Development of new process for treatment of a pharmaceutical wastewater." *Water Science and Technology*, 37, 251-258.

Ryu, J. H., and Beuchat, L. R. (2005). "Biofilm formation by Escherichia coli O157:H7 on stainless steel: Effect of exopolysaccharide and curli production on its resistance to chlorine." *Applied and Environmental Microbiology*, 7, 247- 254.

Sanna Sillankorva, S., Neubauer, P. and Joana Azeredo, J. (2008). "Pseudomonas fluorescens biofilms subjected to phage phiIBB-PF7A." *BMC Biotechnology*, 10, 1186, 1472-6750.

Shotton, D. M. (1989). "Confocal scanning optical microscopy and its applications for biological specimens." *Cell Science*, 94, 175-206.

Sihorkar, V., and Vyas, S. P. (2001). "Biofilm consortia on biomedical and biological surfaces: Delivery and targeting strategies." *Pharmaceutical Research*, 18, 1254–1427.

Sillankorva, S., Oliveira, D. R., Vieira, M. J., Sutherland, I. W., and Azeredo, J. (2004). "Bacteriophage Φ S1 infection of *Pseudomonas* fluorescens planktonic cells versus biofilms." *Biofouling*, 20, 133–138.

Simoes, M., Simoes, L. C., and Vieira, M. J. (2010). "A review of current and emergent biofilm control strategies." *LWT - Food Science and Technology*, 43, 573–583.

Singh, P. K., Schaefer, A. L., Parsek, M. R., Moninger, T. O., Welsh, M. J., and Greenberg, E. P. (2000). "Quorum-sensing signals indicate that cystic fibrosis lungs are infected with bacterial biofilms." *Nature*, 407**,** 762–64.

Smith, W. A. (2005). "Biofilms and antibiotic therapy: Is there a role for combating bacterial resistance by the use of novel drug delivery systems?" *Advanced Drug Delivery Reviews*, 57, 1539– 1550.

SooPark, M., Jung, S. R., Lee, K. H., Lee, M. S., Do, J. O., Kim, S.B. and Bae, K. S. (2006). "Chryseobacterium soldanellicola sp. nov. and Chryseobacterium taeanense sp. nov., isolated from roots of sand-dune plants." *System and Evolutionary Microbiology*, 56, 433-438.

Späth, R., Flemming, H. C., and Wuertz, S. (1998). "Sorption properties of biofilms." *Water Science and Technology*, 37, 207-210.

Börjesson, S., Matussek, A., Melin, S., Löfgren, S., and Lindgren, P.E. (2009). "Methicillin-resistant Staphylococcus aureus (MRSA) in municipal wastewater: an uncharted threat?" *Journal of Applied Microbiology*, 108, 1244-1251.

Stewart, P. S., and Costerton J. W. (2010). "Antibiotic resistance of bacteria in biofilms." *International Journal of Antimicrobial Agents*, 35, 322-32.

Sulakvelidze, A. (2005). "Phage therapy: An attractive option for dealing with antibiotic-resistant bacterial infections." *Drug Discovery Today*,10 , 807–809.

Suttle, C. A.(2005). "Viruses in the sea." *Nature*, 437, 356-361.

Tsien, R.Y., Rink, T.J., and Poenie, M. (1985). "Measurement of cytosolic freee Ca^{2+} in individual small cells using fluorescence microscopy with dual excitation wavelengths." *Cell Calium*, 6, 145-157.

Uchiyama, J., Rashel, M., Matsumoto, T., Sumiyama, Y., Wakiguchi, H., and Matsuzaki, S. (2009). "Characteristics of a novel Pseudomonas aeruginosa bacteriophage, PAJU2, which is genetically related to bacteriophage D3." *Virus Research*, 139, 131-134.

Veran, J. (2002). "Biofouling in food processing: Biofilm or biotransfer potential?" *Food and Bioproducts Processing*, 80, 292–298.

Vieira, M. J., Melo, L., and Pinheiro, M. M. (1993). "Biofilm formation: Hydrodynamic effects on internal diffusion and structure." *Biofouling*, 7, 67–80.

Wilks，S. A., Michels，H., and Keevil，C. W. (2005). "The survival of Escherichia coli O157 on a range of metal surfaces International." *Journal of Food Microbiology*, 105, 445- 454.

Wommack, K. E. and Colwell, R. R. (2000). "Virioplankton: viruses in aquatic ecosystems." *Microbiology*, 64, 69-114.

Yamaguchi, T., Ishida, M., and Suzuki, T. (1999). "Biodegradation of hydrocarbons by Prototheca zopfii in rotating biological contactors." *Process Biochemistry*, 35, 403-409.

Zilouei, H. et al. (2006). "Influence of temperature on process efficiency and microbial community response during the biological removal of chlorophenols in a packed-bed bioreactor." *Applied Microbiology Biotechnology*, 72, 591-599.